



**TWO AXIS DIRECTION FINDING ANTENNA SYSTEM USING
DIFFERENCE – SUM PATTERNS IN X-BAND**

by

SARMAD AHMED SHAIKH

Submitted to the Graduate School of Engineering and Natural Sciences

in partial fulfillment of

the requirements for the degree of

Master of Science

Sabancı University, Turkey

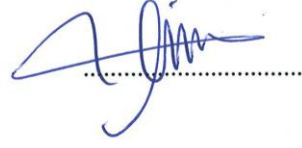
January, 2015

TWO AXIS DIRECTION FINDING ANTENNA SYSTEM USING
DIFFERENCE – SUM PATTERNS IN X-BAND

APPROVED BY:

Prof. Dr. Ibrahim TEKIN

(Thesis Supervisor)



Assoc. Prof. Dr. Ozgur GURBUZ



Assoc. Prof. Dr. Gullu Kiziltas SENDUR



DATE OF APPROVAL: 05/01/2015

TWO AXIS DIRECTION FINDING ANTENNA SYSTEM USING DIFFERENCE – SUM PATTERNS IN X-BAND

Sarmad AHMED

EE, MS THESIS, 2015

Thesis Supervisor: Prof. Dr. Ibrahim Tekin

Keywords: Microstrip Patch Antenna, Antenna Array, Direction of Arrival Systems and Rat Race Ring Coupler.

Abstract:

This thesis work proposes the direction finding antenna system in two axis (θ, ϕ) in x-band (8 to 12 GHz) using difference (Δ) and sum (Σ) patterns of received signal. Direction finding system is constructed using microstrip patch antennas array and 180° hybrid rat race ring coupler which generates Δ and Σ of two received RF signals. Individually, both coupler circuit and antenna elements are optimized in terms of feed location and size using ADS electromagnetic simulation software. In this work, 10 GHz frequency of operation is chosen.

Initially, direction of arrival (DOA) is obtained in one axis (θ) using the patterns of Δ and Σ ports of antenna array of two elements. Using the equations of Δ and Σ of two input signals, radiation patterns at different θ values have been observed in simulation and compared with measured pattern values of constructed circuit. By taking the ratio of Δ to Σ patterns, DOA has been estimated of designed circuit. Later, another DOA circuit in other direction (ϕ) is constructed and DOA has been estimated. By taking the 3D patterns of each circuit in anechoic chamber, both of these circuits are simulated and measured for performance; and from -40 to +40 degrees DOA has been observed with rms error of less than 5 degree in both axis with phi angle from 0 to 180 degrees. Another circuit which combines all these four antennas into one system also has been simulated.

At 10 GHz operating frequency, experimental results using material RT Duroid 5880 ($\epsilon_r = 2.2$, *thickness* = 1.575mm) show that satisfactory performance can be achieved with proposed setup.

FARK VE TOPLAM YAPISI KULLANARAK İKİ EKSENDE YÖN BULUCU X-BAND ANTEN SİSTEMİ

Sarmad AHMED

EM, Yüksek Lisans Tezi, 2015

Tez Süpervizörü: Prof. Dr. İbrahim Tekin

Anahtar Kelimeler: Mikroşerit Yama Anten, Anten Dizisi, Geliş Yönü Sistemleri ve Rat-Race Halka Eşleyicisi.

Özet:

Bu tez, gelen sinyalin farkını (Δ) ve toplamını (Σ) kullanarak X bandında (8-12 GHz) iki ekseninde (θ, \emptyset) yön bulucu anten sistemi sunmaktadır. Yön bulucu sistem, mikroşerit yama antenleri ve gelen RF sinyalin Δ ve Σ 'ını alan rat-race halka eşleyicisinden oluşur. Bireysel olarak, hem eşleyici devre hem de anten elemanları ADS elektromanyetik simülasyon yazılımı kullanılarak besleme yeri ve boyut bakımından optimize edilmiştir. Bu projede, çalışma frekansı 10 GHz olarak belirlenmiştir.

Başlangıç olarak, iki antenden oluşan anten dizisinin Δ ve Σ portlarını kullanarak tek ekseninde (θ) sinyalin geliş yönü (SGY) bulunur. İki girdi sinyalinin Δ ve Σ denklemleri kullanılarak, farklı θ değerlerindeki yayılım yapısı simülasyonda gözlemlenir ve üretilen devrenin ölçümlerinden elde edilen yayılım yapılarıyla karşılaştırılır. Δ 'ın Σ 'a oranı hesaplanarak, tasarlanan devreden SGY öngörülür. Yankısız odada 3 boyutlu sinyal yapılarına bakılarak, her iki devre de simüle edildi ve ölçüldü; aynı zamanda -40° 'den $+40^\circ$ 'lik açıya kadar 5° 'den daha az bir ortalama karekök (RMS) hatasıyla ve her iki ekseninde 0° 'den 180° 'ye kadar ϕ açısıyla SGY gözlemlendi. Bütün bu dört anteni içeren başka bir devre de ayrıca simüle edildi.

10 GHz çalışma frekansında, RT Duroid 5880 ($\epsilon_r = 2.2$, *kalınlık* = 1.575mm) malzemesi kullanılarak elde edilen deney sonuçları gösterdi ki önerilen kurulum ile tatmin edici performans parametrelerine ulaşılabilir.

Acknowledgements

First of all I would like to acknowledge my thesis supervisor Dr. Ibrahim Tekin and would like to thank and express my deepest gratitude for his valuable guidance, support, continuous encouragement and keeping me motivated all the time. It is a wonderful experience and honor for me to work with him for entire my masters degree. Specially I would like to appreciate his instantly help, patience and encouragement during the thesis work.

I am also thankful to my dissertation jury members, Dr. Orguz Gurbuz and Dr. Gullu Kiziltas for spending their valuable time to judge my thesis.

I would like to acknowledge Higher Education Commission (HEC), Pakistan for their great co-operation and by keeping trust to award me full funded scholarship to obtain Masters degree at Sabanci University, Turkey.

I also cannot stay away to myself to acknowledge my lovely lab fellows PhD students, Haq Nawaz and Mir Mehdi for their wonderful and appreciable assistance for my asked questions and specially during the fabricated circuits measurements performed in Anechoic chamber.

Last but not least, I would like to say bundles of thanks to my family and friends for their endless morally support in every step during my academic life.

Dedicated to my late father Gul Mohammad.....

©Sarmad AHMED 2015

All Rights Reserved

TABLE OF CONTENTS

| | |
|--|-----------|
| 1. INTRODUCTION | 1 |
| 2. BACKGROUND | 4 |
| 2.1 DOA SYSTEM | 4 |
| 2.2 ANTENNA BASICS AND ITS PARAMETERS | 6 |
| 2.2.1 DIRECTIVITY AND GAIN OF ANTENNA | 8 |
| 2.2.2 REFLECTION COEFFICIENT (Γ) AND RETURN LOSS (RL) | 9 |
| 2.2.3 3DB BEAMWIDTH | 9 |
| 2.2.4 BANDWIDTH..... | 9 |
| 2.3 MICROSTRIP ANTENNAS | 9 |
| 2.3.1 MICROSTRIP PATCH ANTENNAS | 10 |
| 2.3.2 DESIGN PROCEDURE | 11 |
| 2.3.3 MICROSTRIP PATCH ANTENNA FORMULATIONS | 13 |
| 2.3.4 ADS SIMULATION OF 10GHZ MICROSTRIP PATCH ANTENNA | 15 |
| 2.3.5 MICROSTRIP ANTENNA ARRAYS..... | 19 |
| 3. RAT RACE COUPLER | 22 |
| 3.1 180 ⁰ HYBRID RING COUPLER DESIGN | 23 |
| 4. DOA FINDING SYSTEM DESIGN AND EXPERIMENTAL RESULTS | 30 |
| 4.1 $\Delta - \Sigma$ PATTERN ANALYSIS THROUGH MATLAB CODING | 30 |
| 4.2 ESTIMATING DOA IN THETA (Θ) AXIS | 31 |
| 4.3 ESTIMATING DOA IN PHI (Φ) AXIS | 40 |
| 5. CONCLUSION | 51 |
| 6. APPENDICES | 53 |
| 6.1 APPENDIX A | 53 |
| 6.2 APPENDIX B | 56 |
| 6.3 APPENDIX C | 57 |
| 7. REFERENCES | 59 |

LIST OF FIGURES

| | |
|---|----|
| FIGURE 2-1: BLOCK DIAGRAM OF DOA SYSTEM | 5 |
| FIGURE 2-2: TYPICAL PATTERN OF DIFFERENCE AND SUM PORTS..... | 6 |
| FIGURE 2-3: ANTENNA IMPEDANCE VERSUS FREQUENCY, SHOWING RESONANCE FREQUENCY | 8 |
| FIGURE 2-4: BASIC MICROSTRIP PATCH ANTENNA DESIGN | 11 |
| FIGURE 2-5: DIFFERENT PATCH ANTENNA DESIGNS WITH MATCHING TECHNIQUES | 12 |
| FIGURE 2-6: BASIC GEOMETRY OF QWT FED MICROSTRIP PATCH ANTENNA | 13 |
| FIGURE 2-7: TL MODEL OF MICROSTRIP PATCH ANTENNA | 14 |
| FIGURE 2-8: LINECALC PARAMETERS FOR RT DUROID 5880 | 17 |
| FIGURE 2-9: LAYOUT DESIGN OF 10 GHZ PATCH ANTENNA..... | 17 |
| FIGURE 2-10: S11 OF DESIGNED 10GHZ PATCH ANTENNA..... | 18 |
| FIGURE 2-11: ANTENNA PARAMETERS OF DESIGNED 10 GHZ PATCH ANTENNA | 18 |
| FIGURE 2-12: 3D RADIATION PATTERN OF DESIGNED 10GHZ PATCH ANTENNA..... | 19 |
| FIGURE 2-13: 2D GAIN AND RADIATED POWER PLOTS OF DESIGNED 10GHZ PATCH ANTENNA..... | 19 |
| FIGURE 2-14: 4-ELEMENT PATCH ARRAY | 20 |
| FIGURE 3-1: TYPICAL RAT RACE RING COUPLER DESIGN | 22 |
| FIGURE 3-2: SCHEMATIC DESIGN OF 180 ⁰ HYBRID RAT RACE RING COUPLER | 24 |
| FIGURE 3-3: SCHEMATIC S11, S22, S33 AND S44 OF PORT1, PORT2, PORT3 AND PORT4 | 24 |
| FIGURE 3-4: PORT ISOLATIONS | 25 |
| FIGURE 3-5: 180 ⁰ PHASE DIFFERENCE IN BETWEEN TWO INPUT SIGNALS AT PORTS 3 AND 4 | 25 |
| FIGURE 3-6: TWO INPUT SIGNALS ARRIVING IN PHASE AT SUM PORT | 26 |
| FIGURE 3-7: LAYOUT DESIGN OF RAT RACE COUPLER AT 10 GHZ CENTRAL FREQUENCY | 27 |
| FIGURE 3-8: LAYOUT S11,S22,S33,S44 OF PORTS 1,2,3,4 RESPECTIVELY | 27 |
| FIGURE 3-9: PORT ISOLATIONS | 28 |
| FIGURE 3-10: 180 ⁰ PHASE DIFFERENCE IN BETWEEN TWO INPUT SIGNALS AT PORTS 3 AND 4..... | 28 |
| FIGURE 3-11: TWO INPUT SIGNALS ARRIVING IN PHASE AT SUM PORT | 29 |
| FIGURE 4-1: NUMERICALLY OBTAINED Δ AND Σ PATTERNS | 30 |
| FIGURE 4-2: ADS LAYOUT DESIGN OF Δ - Σ PATTERN, CIRCUIT 1 (THETA AXIS) | 32 |
| FIGURE 4-3: S-PARAMETERS OF Δ AND Σ PORTS, SIMULATED IN ADS LAYOUT | 33 |
| FIGURE 4-4: FAR FIELD PATTERN AT 0 DEGREE..... | 34 |
| FIGURE 4-5: ANTENNA PARAMETERS | 34 |
| FIGURE 4-6: DIFFERENCE – SUM PATTERN CIRCUIT 1 FABRICATED (THETA AXIS)..... | 35 |
| FIGURE 4-7: TESTING THE CIRCUIT IN ANECHOIC CHAMBER WITH HORN ANTENNA | 36 |
| FIGURE 4-8: MEASURED S-PARAMETERS OF Σ AND Δ PORTS, RESPECTIVELY | 36 |
| FIGURE 4-9: MEASURED NORMALIZED Δ AND Σ PATTERNS OF CIRCUIT 1 | 37 |
| FIGURE 4-10: MEASURED ANGLE OF ARRIVAL OF RECEIVED SIGNAL OF CIRCUIT1 (THETA AXIS).. | 37 |

| | |
|--|----|
| FIGURE 4-11: PLOTS OF ESTIMATED AOA -40^0 TO 40^0 IN THETA AXIS AT DIFFERENT PHI VALUE . | 38 |
| FIGURE 4-12: RMS ERROR FOR MEASURED DOA IN THETA AXIS (-40^0 TO $+40^0$) | 39 |
| FIGURE 4-13: RMS ERROR AT DIFFERENT DOA RANGES IN THETA AXIS..... | 39 |
| FIGURE 4-14: ADS LAYOUT DESIGN OF Δ - Σ PATTERN, CIRCUIT 2 (HORIZONTAL) | 41 |
| FIGURE 4-15: S-PARAMETERS OF Δ AND Σ PORTS, SIMULATED IN ADS LAYOUT | 41 |
| FIGURE 4-16: FAR FIELD PATTERN | 42 |
| FIGURE 4-17: ANTENNA PARAMETERS | 43 |
| FIGURE 4-18: DIFFERENCE – SUM PATTERN CIRCUIT 2 FABRICATED (PHI AXIS) | 43 |
| FIGURE 4-19: MEASURED S-PARAMETERS OF Σ AND Δ PORTS, RESPECTIVELY OF CIRCUIT 2 | 44 |
| FIGURE 4-20: MEASURED NORMALIZED Δ AND Σ PATTERNS (CIRCUIT 2) | 45 |
| FIGURE 4-21: MEASURED ANGLE OF ARRIVAL OF RECEIVED SIGNAL OF CIRCUIT2 (PHI AXIS) | 45 |
| FIGURE 4-22: PLOTS OF ESTIMATED AOA -40^0 TO 40^0 IN PHI AXIS AT DIFFERENT THETA VALUES | 47 |
| FIGURE 4-23: RMS ERROR FOR MEASURED DOA IN PHI AXIS (-40^0 TO $+40^0$)..... | 48 |
| FIGURE 4-24: RMS ERROR AT DIFFERENT DOA RANGES IN PHI AXIS | 48 |
| FIGURE 4-25: ESTIMATED DOA IN BOTH AXIS (THETA AND PHI) AT FIXED PHI VALUE (0 DEG.) | 49 |
| FIGURE 4-26: OVERALL SYSTEM DESIGN | 50 |

1. Introduction

The objective of this thesis is to design a microstrip patch antenna array with rat race coupler in x-band of frequency to estimate the direction of arrival (DOA) or the angle of arrival (AOA) of received signal. Main motivation behind the antenna array and rat race coupler system is to find the direction of received signal in two axis using the sum (Σ) and difference (Δ) patterns at 10 GHz operating frequency. As part of the array section across a microstrip patch antenna is designed as the receiving element of RF signal. Further, rat race coupler is designed and optimized at the central frequency in order to obtain accurate sum and difference of two received signals.

The direction of arrival estimation system having applications in radar, sonar, military, acoustic, communications and medical imaging, is an omnipresent task in array signal processing [1]. Recently developed a great number of radar and sensor systems require high efficiency, functionality and compactness [2]. One of the efficient methods of improving the quality of received signal is to find the DOA of the signal by targeting the reception only on the expected direction and rejecting the interferer reception from other directions [3]. Hence the main objective of DOA system is to define a function which finds the AOA of received signal. Many publications have studied the DOA system design and its characteristics which suggest different types of algorithms to estimate the direction of received signal. The techniques used in literature in finding the DOA are generally complex and their focus is mainly in one axis only.

The focus of this thesis is to find the DOA of received signal in x-band (10 GHz) frequency in two axis (θ and ϕ) using the difference and sum patterns of most popular 180° hybrid rat race ring coupler. System design includes two antenna arrays placed in two directions (vertical and horizontal) each consists of two microstrip patch antennas operating at 10 GHz frequency, rat race ring coupler providing the difference and sum of two received RF signals; and feeding network. When two signals are received by two antenna elements of an array, these two signals are applied to the two input ports of 4 ports ring coupler which generates difference (Δ_1) and sum (Σ_1) on two output ports. Using the difference and sum patterns of coupler, direction of arrival of received signal is estimated in one axis (θ) using the AOA function which is explained in details in section (4) of this thesis. For the sack of clear understanding, let's call this part of design as circuit 1 (in vertical direction). Similarly, another same part of design is constructed which is at 90° of first circuit and let's call it as circuit 2 (in horizontal direction) which provides difference (Δ_2) and sum (Σ_2) patterns of two received signals. By applying DOA function on obtained patterns as done in circuit 1, DOA in second axis (ϕ) has been obtained. All this work is first simulated and tested on

Advanced System Design (ADS) momentum software and then constructed on RT Duroid 5880 material.

Each part of the system is designed and tested on ADS software separately and optimized to the desired range of expected results. Initially microstrip patch antenna was designed at 10 GHz central frequency and input impedance was matched using quarter wave transformer method. This designed patch antenna was analyzed carefully which in result provided better S-parameters, gain, directivity and radiation pattern. In Matlab, by multiplying the radiation pattern (gain plot) of this single patch antenna with the equations of sum and difference, radiation patterns of both Σ and Δ are analyzed numerically. This part of the design is well explained in next section (4). After getting good design of patch antenna, array of two antenna elements was implemented using 0.6λ spacing in between two elements where $\lambda = 30$ millimeter (mm) is free space wavelength at 10 GHz frequency at the speed of light ($v = 3 \times 10^8$ meter/second). In order to get the Σ and Δ of two received signals from two antenna elements of array, 180° hybrid rat race ring coupler was designed separately at 10 GHz and optimized for the desired outputs. Complete studies regarding rat race coupler is discussed in section (3). All parts of the system are very carefully designed and optimized in ADS momentum software to get the proper results.

Having simple structure of array of two elements of patch antennas and ring coupler, system design is much straight forward and able to provide the direction of arrival of received signal using difference and sum patterns. However, it has been investigated that transmission lines of 50Ω at 10 GHz produces mutual coupling if passing near the patch antenna or coupler which consequently disturbs the patterns of sum and difference ports. Therefore, good care was given in transmission lines design which resulted in better Σ and Δ patterns.

The thesis is organized as follows:

Chapter 1: This section of thesis provides the introduction to the thesis work, objective, approach and scope of the work.

Chapter 2: Gives essential background about DOA system and covers the literature review on microstrip patch antennas and array design. For this thesis work, 10 GHz patch antenna is designed and investigated in this section.

Chapter 3: Analyzes the 4 ports 180° hybrid rat race ring coupler. It is well investigated through ADS layout and schematic simulations.

Chapter 4: Discusses the complete design both in hardware and software format of direction finding system. Also gives the results obtained from simulations and measurements of the system design.

Chapter 5: Concludes the work of this thesis done.

Chapter 6: Gives appendices about supplementary and necessary formulations and Matlab codes.

2. Background

2.1 DOA System

Efficiently estimating the direction of received signal has remained challenging task in radar, military and communication systems working in x-band of frequency. It is necessary to focus the reception in estimated direction and rejecting in all other directions which in result increases the quality of received signals. There exist many algorithms in finding the DOA such as sensor array, Bartlett method, Capon method, MUSIC algorithm, etc [1][3]. But these algorithms are generally complex and depending on number of antennas employed and their parameters such as spacing between them, gain and directivity; number of users, geographical position, and number of sample signals taken in estimating process [4].

It is known that there exist one to one relationship between direction of a signal and the associated received steering vector [5]. It is therefore possible to estimate the direction of received signal by inverting this relationship. So in this thesis work a novel antenna system using difference (Δ) and sum (Σ) patterns of received 10 GHz signal is proposed. This proposed DOA finding system consists of microstrip patch antenna array, rat race ring coupler and feeding network. Block diagram of simple DOA system is shown in figure 2-1.

Received signals of antenna array elements are fed to two input ports of 4-ports 180° hybrid rat race ring coupler which generates the difference (Δ) and sum (Σ) of two received signals at two output ports. Coupler produces the Δ and Σ of the fed signals according to the following equations, respectively:

$$\Delta = 1 - e^{-jk d \sin \theta} \quad (2-1)$$

$$\Sigma = 1 + e^{-jk d \sin \theta} \quad (2-2)$$

Using this pattern of Δ and Σ , angle of arrival is derived by taking the ratio Δ to Σ . After performing some mathematical iteration, AOA can be estimated as given in following equation (2-3) [2].

$$\theta = \sin^{-1} \left(\frac{\lambda}{\pi d} \tan^{-1} \frac{\Delta}{\Sigma} \right) \quad (2-3)$$

where λ is free space wavelength, d is spacing between two antenna elements, Δ and Σ are the subtracted and summed amplitudes of RF signals received by antenna array of two elements.

Typical patterns of difference and sum ports of coupler as given in [2] are shown in figure (2-2) in order to take in account as pre-requirement of coupler's output.

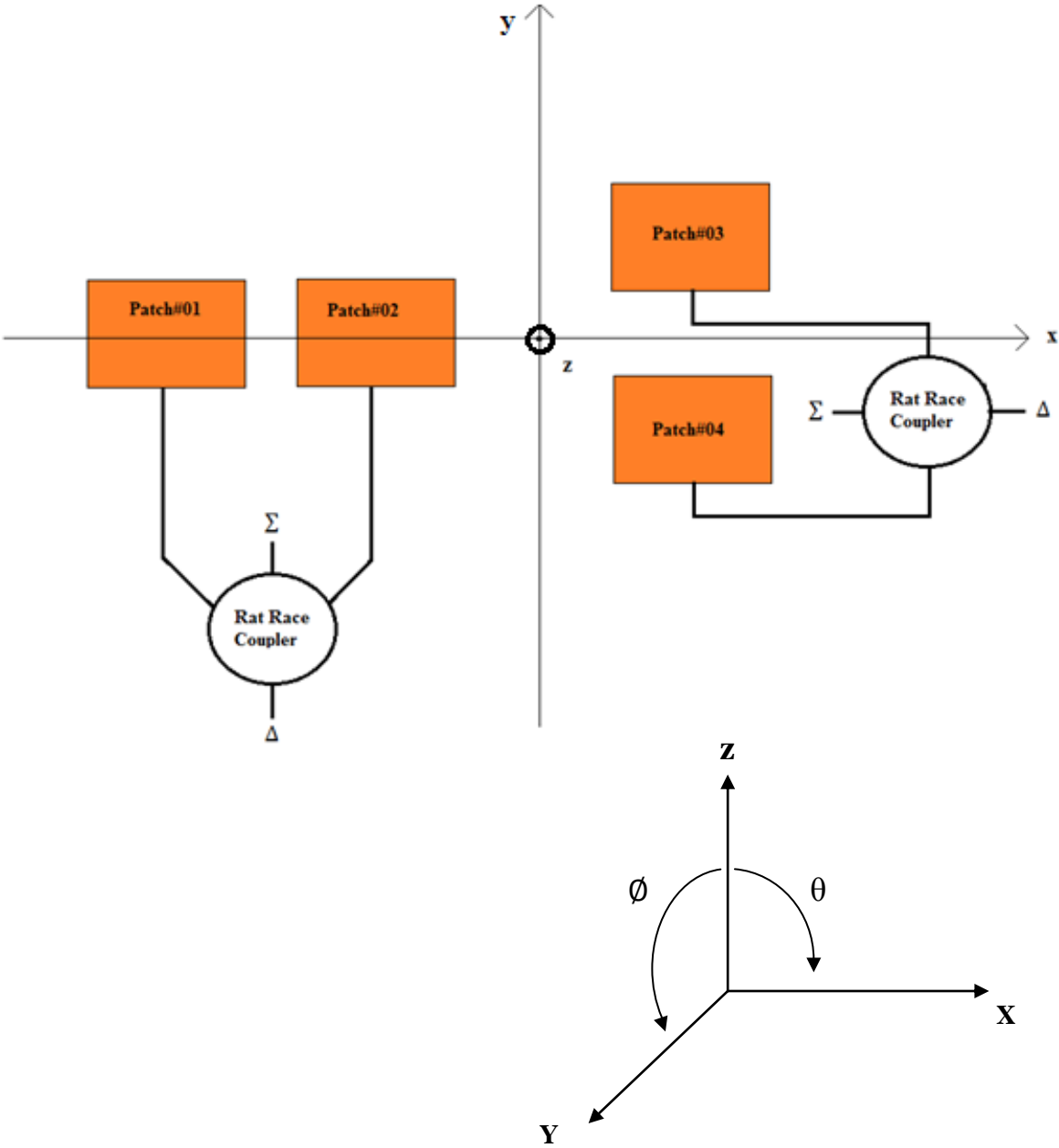


Figure 2-1: Block diagram of DOA System

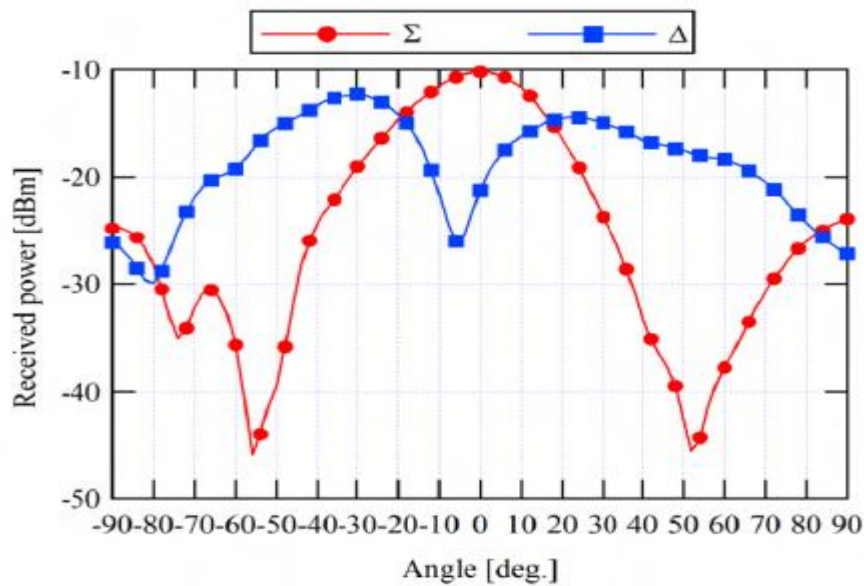


Figure 2-2: Typical pattern of difference and sum ports [6].

2.2 Antenna Basics and its Parameters

Antenna is a device also often called radiant, designed to transmit or receive electromagnetic energy by matching these sources of energy and the space. Note that the same antenna can be used to transmit or receive the radio signals.

As mentioned in [7], in addition to transmitting and receiving the electromagnetic energy, an antenna in an advanced wireless system is usually required to optimize or accentuate the radiation energy in some particular directions and block it in other directions. Therefore, antenna can also be used for any required direction as well. Antenna in its physical form can be a piece of conducting wire, a copper patch, an aperture, an assembly of many elements (array), a reflector, a lens, and so forth (note that here in this work only patch antenna will be discussed in details). So an *antenna* being a device used for converting electromagnetic radiation in space into electrical currents in conductors or vice-versa, depending on whether it is being used for receiving or for transmitting, respectively, is usually easier to calculate the properties of transmitting antennas. Fortunately, most properties of a transmitting antenna remain unchanged when the antenna is used in receiving mode. Often the same analysis of a transmitting antenna is carried to understand a receiving antenna used in radio astronomy.

The information which is supposed to be sent is varied, for example through some kind of digital/analogue modulation scheme and treatment, and still conveyed or guided by a cable to the antenna. The antenna then starts its work and radiates this information through a medium (usually air) until it reaches the other receiving antenna, which in this case will make receiving the signal, making it still the way the cable to the device that will make such demodulation (and other treatments), recovering the original information. There also occurs some path losses and attenuation of signals which degrades the received signal quality.

Antenna is usually made of metallic material (aluminum / brass) and metal itself is formed by atoms. When all atoms are brought together to make metal then there is a set of free electrons which start to move when a voltage is applied. Motion of these electrons on antenna creates electromagnetic radiation in the form of radio waves. Electromagnetic waves transmitted from transmitting antenna travel in free space medium and reach at receiving antenna which again convert the electromagnetic waves into electrons and make them to vibrate same as in transmitter which in turn results in generating the current corresponding to the transmitted information.

While talking about electromagnetic waves, another important concept is the polarization which is very important to be considered while designing the antennas, i.e., what is the plane of the electrical component of the field in which the wave propagates. In [5] and [8], it is well explained that electromagnetic waves are composed of two planes, vertical and horizontal. These planes represent the electric and magnetic fields and these components are always orthogonal, vectors off by 90 degrees. They vary in phase or zero degrees of electrical phase shift. So in short, depending on how the signal coupling is done - the antenna is oriented - we have a definition of polarization. The concept of polarization is very important in antennas, mainly because when a signal is transmitted in one polarization must be received in the same polarization, otherwise we will have an attenuation (loss), known as cross-polarization.

Apart from polarization, there is also an important concept in antenna phenomenon called 'resonance or operating frequency'. Resonance is the phenomenon that occurs in a particular frequency where we have a maximum possible transfer of energy in that particular defined frequency. In the case of antennas, for there to be resonance, its size (physical length) must be a multiple of the wavelength of the transmitted/received signal. In this case, we will have a main frequency where the antenna delivers the maximum amount of energy possible - resonant. The larger the size (length) of elements of antenna, lower the resonant frequency and vice versa [8]. In more technically terms it can be described that resonance is where the inductance and capacitance reactance cancel each other and we have pure resistive impedance as shown in following figure 2-3.

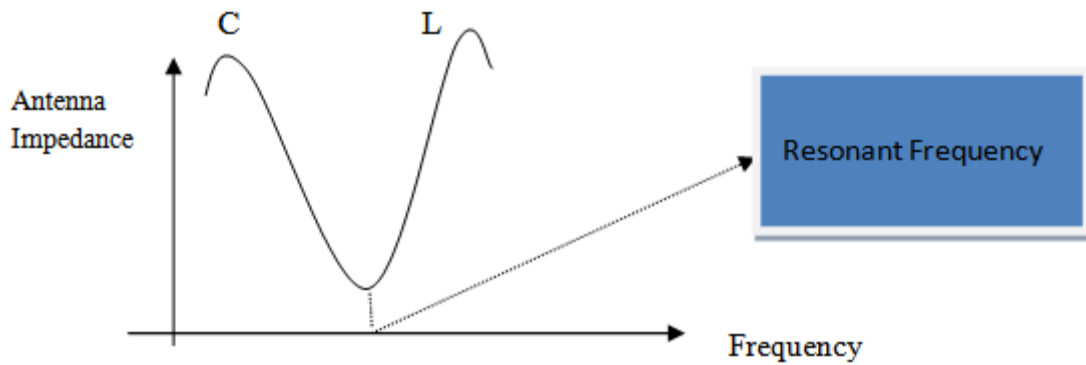


Figure 2-3: Antenna Impedance versus Frequency, showing the resonance frequency

Following are the most important parameters to be analyzed when designing any type of antenna.

2.2.1 Directivity and Gain of Antenna

One of the most important parameters of antenna to measure is that how much it concentrates the energy in a particular direction in preference to radiation in other directions. This characteristic of antenna is called directivity and is equal to its power gain if it is 100% efficient and mathematically is given by:

$$D = \frac{4\pi}{\Omega_A} \quad (2 - 4)$$

Directivity: can also be defined as the ratio of radiation intensity in a certain direction to the average radiation intensity, as given by equation (2) [1].

$$D(\theta, \phi) = \frac{U(\theta, \phi)}{U_{ave}} \quad (2 - 5)$$

Gain: When an antenna is used in a system for example in a transmitting antenna, we are actually interested in how efficiently the antenna transfers the available power at its input terminals to its radiated power, together with its directivity properties. Therefore, gain is used to quantify this and is defined as 4π times the ratio of radiation intensity in a given direction to the net power accepted by antenna from the connected transmitter, as given in equation (2.6) [2].

$$G(\theta, \phi) = \frac{4\pi U(\theta, \phi)}{P_{in}} \quad (2 - 6)$$

2.2.2 Reflection Coefficient (Γ) and Return Loss (RL):

Reflection coefficient is defined to give ratio between reflected wave and incident wave. Transmission lines have a resistance related with it which is called characteristics impedance, denoted with Z_0 . When transmission line is terminated with an arbitrary load which has not same impedance as of transmission line then wave is reflected back and power is not transmitted properly. Reflected wave is given by following relation:

$$\Gamma = \frac{Z_l - Z_0}{Z_l + Z_0} \quad (2 - 7)$$

Return loss is the parameter that shows the amount of power that is reflected due to the impedance mismatch between the source and the load and is given by:

$$RL = -20\log |\Gamma| \text{ (dB)} \quad (2 - 8)$$

2.2.3 3dB Beamwidth:

In addition to directivity, the radiation patterns of the antenna are also characterized by their beamwidths and sidelobe levels. Some numerical aspects of the antenna pattern properties can be defined after antenna pattern is plotted. Half-power beamwidth or 3dB beamwidth is the measure of the angular width of the -3dB points on the antenna pattern relative to maximum level.

Direction where the maximum radiations are obtained is called the **main beam/lobe** while smaller beams which can never be completely eliminated are away from the main beam and are called **side lobes** and usually occur in undesired direction. Another commonly quoted beamwidth is the null to null beamwidth. This is the angular separation from which the magnitude of the radiation pattern decreases to zero (negative infinity dB) away from the main beam [9].

2.2.4: Bandwidth:

Defines the range of frequency over which antenna meets certain performance criteria. It is generally defined through the return loss of the antenna for the frequency band in which return loss is less than -10dB.

2.3 Microstrip Antennas

Microstrip antennas or Printed antennas are constructed using printed circuit fabrication techniques such that a portion of the metallization layer is used to radiate the electromagnetic energy in space. Microstrip patch elements and arrays of patches are the most types of printed antenna and were conceived in 1950s [10]. This type of

antenna got much attention in 1970s and in turn it showed remarkable results with many useful design configurations. Patch antennas are much popular among antenna engineers because of their low profile, for the ease with which these antennas can be configured to specialized geometries and also due to one of the promising advantage of their low cost when produced in large quantities [11]. This section explains the basic operating principles of microstrip patch antennas, design procedure and most useful formulas which help to calculate the design parameters of the antenna. Details and derivations of the formulas are given in [5] and [7].

2.3.1 Microstrip Patch Antennas

Microstrip patch antennas which are also called patch antennas are becoming increasingly useful nowadays because they can be printed directly onto a circuit board like any electronic circuit. Patch antennas are getting much popularity and becoming very widespread within the mobile phone market because Patch antennas are:

- low profile
- comfortable to planar and non-planar surfaces
- simple and inexpensive to manufacture
- compatible with MMIC circuit designs
- versatile in frequency, polarization, radiation pattern and impedance

Having such great properties, patch antennas have low efficiency, low power, high Q, narrow bandwidth and spurious radiation (surface waves).

As mentioned in [12], consider the microstrip patch antenna as shown in figure 2-4, fed by a microstrip transmission line. The patch antenna, microstrip transmission line and ground plane are made of high conductivity metal often made of copper. The patch is made of length (L), width (W), and sitting on top of a substrate (some dielectric circuit board) of thickness h with the substrate permittivity ϵ_r . The thickness of the ground plane or of the microstrip is not critically important. Typically the height h is much smaller than the wavelength of operation but not much smaller than 0.05 of a wavelength. Thick substrates with low ϵ_r are desirable for antenna performance, better efficiency, larger bandwidth, larger element size while thin substrates with high ϵ_r are desirable for microwave circuitry. Radiation mechanism is through the fringing fields at the ends of the patch which can be treated as radiating slots. As $w/h \gg 1$ and $\epsilon_r \gg 1$, the electric lines concentrate mostly in the substrate. Note that some of the waves travel in the substrate and some waves travel in the air, so we have effective dielectric constant $\epsilon_{r,eff}$ given by equation (2-9).

$$\epsilon_{\text{eff}} = \frac{\epsilon_r + 1}{2} + \frac{\epsilon_r - 1}{2} \left[1 + 12 \frac{h}{w} \right]^{-1/2} \quad (2-9)$$

According to reference [5], it is the fringing fields that are responsible for the radiation. Note that the fringing fields near the surface of the patch antenna are both in the +y direction. Hence, the fringing E-fields on the edge of the microstrip antenna add up in phase and produce the radiation of the microstrip antenna. The current adds up in phase on the patch antenna as well; however, an equal current but with opposite direction is on the ground plane, which cancels the radiation. This also explains why the microstrip antenna radiates but the microstrip transmission line does not. The microstrip antenna's radiation arises from the fringing fields, which are due to the advantageous voltage distribution; hence the radiation arises due to the voltage and not the current. The patch antenna is therefore a "voltage radiator", as opposed to the wire antennas, which radiate because the currents add up in phase and are therefore "current radiators".

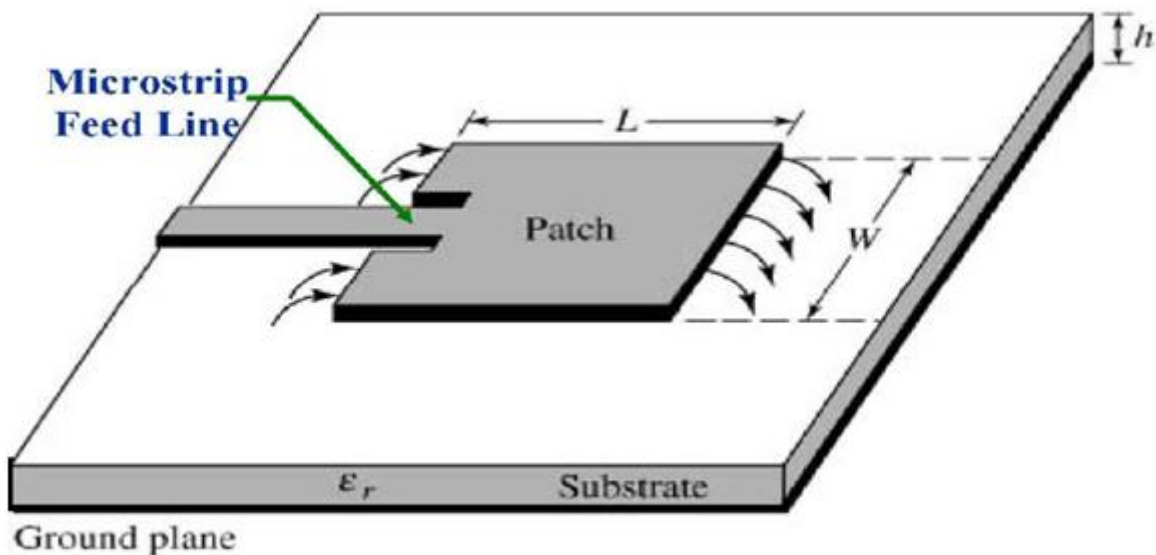


Figure 2-4: Basic microstrip patch antenna design

2.3.2 Design Procedure

The patch antenna belongs to the class of resonant antennas and its resonant behavior is responsible for the actual challenge in this type of antenna design specially obtaining the adequate bandwidth. Conventional patch designs yield bandwidths as low as a few percent [13]. The resonant nature of microstrip antennas also means that at frequencies below UHF they become excessively large in size. Therefore, these antennas are typically used at frequencies range from 1 to 100 GHz. Further it is

discussed in [14] about tradeoff in microstrip antennas that is to design a patch with loosely bound fields extending into space while keeping the fields tightly bound to the feeding circuitry. Therefore, it is necessary to be accomplished with high radiation efficiency and with the desired polarization, bandwidth and impedance.

Many designs exist for microstrip patch antennas with different styles of matching the patch with transmission line, as Probe Feed, Microstrip Edge Feed with Quarter-wave Transformer, Microstrip Edge Feed Inset, Probe Feed with a gap, Microstrip Edge Feed with gap and Two-layer Feed; these all designs taken from [5], are shown in figure 2-5. Figure 2-6 shows the most commonly used microstrip antenna, usually called as *rectangular or square patch* being fed from a microstrip transmission line and matched through quarter wave transformer (QWT) line section. Formulas are available in literature to estimate the resonant length and width of patch and QWT line but empirical adjustments are often necessary in practice. In this thesis, QWT fed microstrip patch antenna is designed and used for antenna part of the DOA system at desired frequency of operation.

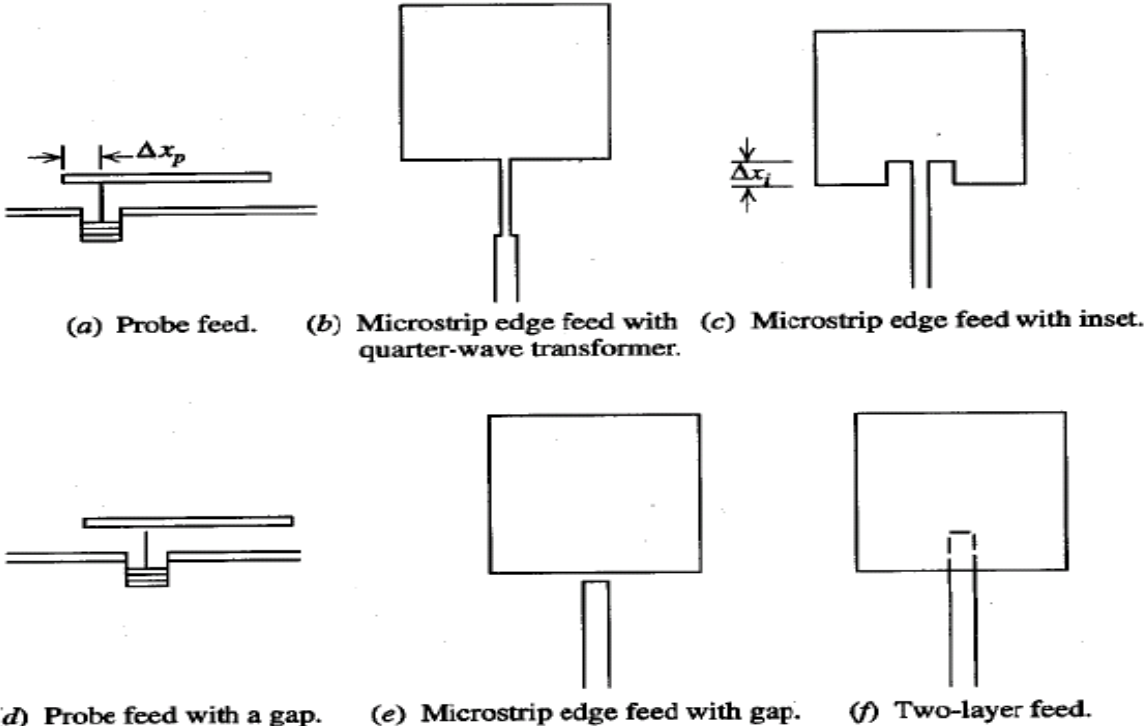


Figure 2-5: Different patch antenna designs with matching techniques [5].

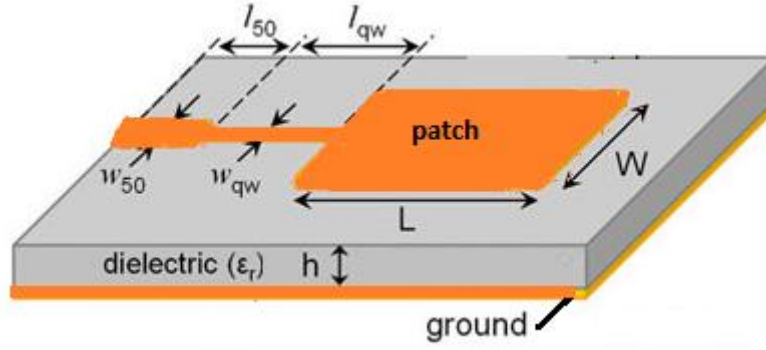


Figure 2-6: Basic geometry of QWT fed microstrip patch antenna

2.3.3 Microstrip Patch Antenna Formulations

There exist many modeling techniques of microstrip antenna. Three widely used techniques are transmission-line, cavity and full-wave models. Transmission-line (TL) having simplest model is easy to implement but with low efficiency. Cavity model having better accuracy but increased complexity is empirical model like TL model that utilizes assumptions to simplify the computations. While the full-wave model computationally expensive provides an exact analysis of Maxwell's equations and potentially provides the best precision because it considers boundary conditions on the dielectric-air periphery.

In TL model the radiation from microstrip patch antennas can be calculated from the equivalent magnetic current distributions around the edges of radiating patch. Magnetic current values can be obtained from edge voltage distributions. Thus for a given excitation and for a specified mode of the resonance of the patch, problem reduces to that of finding the edge voltage distribution. The microstrip patch antenna is modeled as two radiating slots separated by distance L_{eff} . By looking at figure 2-7, physical meaning of this L_{eff} can be understood which is essentially the length of patch denoted by L , plus an additional distance, $2\Delta L$, to account for the fact that electric field of an open microstrip line does not end suddenly while the patch looks larger than its physical dimensions due to fringing fields. While it can either introduce a capacitance or equivalent length extension which is compensated in [7] by following formula.

$$\Delta L = 0.412h \frac{(\epsilon_{reff} + 0.3) \left(\frac{W}{h} + 0.264\right)}{(\epsilon_{reff} - 0.258) \left(\frac{W}{h} + 0.8\right)} \quad (2-10)$$

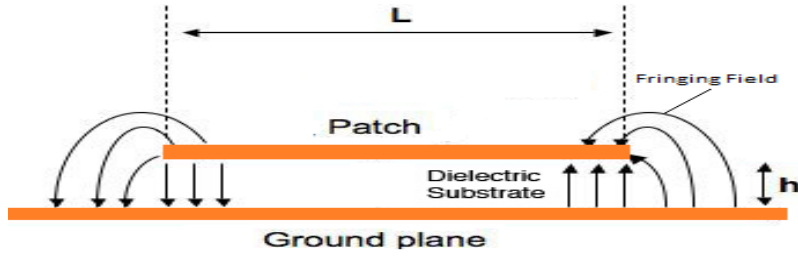


Figure 2-7: TL model of microstrip patch antenna

Here ϵ_{reff} is the effective dielectric constant of microstrip TL which is given in equation (2-9) and its value is slightly less than ϵ_r because the fringing fields around the periphery of the patch are not confined in the dielectric substrate but also spread in the air.

Moreover, length of the patch must be slightly less than $\lambda_g/2$ in order to operate in TM_{10} fundamental mode where λ_g is wavelength in dielectric medium and is given by $\lambda_0/\sqrt{\epsilon_{reff}}$ where λ_0 is free space wavelength. More importantly, width (W) of the patch plays a significant role in the microstrip antennas which requires a deep attention. Small values of width result in low antenna efficiencies while large values lead to the higher order modes. In this case for efficient radiation to obtain, width W is given in [15] as follow:

$$W = \frac{c}{2 \times f_0 \times \sqrt{\frac{(\epsilon_r + 1)}{2}}} \quad (2-11)$$

For input impedance of resonate edge-fed patch, an expression is given in [7] as:

$$Z_A = 90 \frac{\epsilon_r^2}{\epsilon_r - 1} \left(\frac{L}{W}\right)^2 \Omega \quad \text{half-wave patch} \quad (2-12)$$

To find out the characteristic impedance of the matching section QWT as shown in previous figure (2-6), we have

$$Z_0' = \sqrt{Z_0 \times Z_A} \quad (2-13)$$

Length of QWT section is $l_{qw} = \lambda/4$ m.

The radiation pattern of the rectangular microstrip patch antenna for the TM_{10} mode could be calculated by combining the radiation pattern of the two slots of length ΔL and width W on the infinite ground plane, which are spaced at a distance $L + \Delta L$. Simple expressions exist as given in [7] which approximate the radiation patterns of the rectangular microstrip patch antenna and are given below.

$$E_{\theta} = E_0 (\cos\phi)f(\theta, \phi) \quad (2-14)$$

$$E_{\phi} = -E_0(\cos\theta)(\sin\phi)f(\theta, \phi) \quad (2-15)$$

$$f(\theta, \phi) = \frac{\sin\left(\frac{kW \sin(\theta)\sin(\phi)}{2}\right)}{\frac{kW \sin(\theta)\sin(\phi)}{2}} \cos\left(\frac{kL\sin(\theta)\cos(\phi)}{2}\right) \quad (2-16)$$

where first part of the equation (2-16) is the pattern factor for a uniform line source with length w and second part is corresponding to the array factor for two equally excited elements having space L . To write the principle plane patterns, further simplifications can be made, as given in [7].

$$F_{E\theta} = \cos(\beta L \sin(\theta)/2) \quad (2-17)$$

$$F_{H\theta} = \cos(\theta) \frac{\sin\left(\frac{\beta \omega \sin(\theta)}{2}\right)}{\frac{\beta \omega \sin(\theta)}{2}} \quad (2-18)$$

where θ is measured angle from the broadside.

2.3.4 ADS simulation of 10GHz microstrip patch antenna

After studying theoretical concepts, its good idea to design a patch antenna in any antenna software, in order to verify the studied formulas of microstrip patch antenna. Various types of softwares exist for antenna designing, such as High Frequency Structure Simulator (HFSS), Advanced Design System (ADS), Numerical Electromagnetic Code (NEC), Computer Simulation Technology (CST), etc. In this thesis ADS software is used for simulation purpose. ADS momentum software is a full-wave electromagnetic simulator based on the method of moments (MOM) and is used to simulate the structure of the antenna. Antenna of interest is designed in the layout part of the ADS of desired dimensions. Layout is composed of two layers, one is patch layer and other is ground layer. Using internal port, patch feeding is obtained and ground reference port to the internal port is defined at the ground layer.

Here, a patch antenna design at resonate frequency of 10GHz is given which will be used further in desired DOA system. Before designing any required frequency antenna, it is mandatory to select a dielectric substrate (ϵ_r) on which patch will be drawn because all calculations depend on the properties of substrate, such as its permittivity ϵ_r value, tangent loss, thickness 'h', conducting layer thickness 't' (as copper), air value, etc. In this work, RT Duroid 5880 substrate is used throughout the

design and copper is used as conducting layer over the substrate. Substrate properties are given in table 1.

Table 1: RT Duroid 5088 substrate properties

| | |
|-------------------------------------|-----------------------|
| Substrate permittivity ϵ_r | 2.2 |
| Substrate Thickness h | 1.575 mm |
| Substrate Tangent Loss | 0.0004 |
| Copper Conductivity | 5.8×10^7 S/m |
| Copper Thickness t | 17 μm |

Having substrate values and desired frequency of operation (f_0), other required parameters such as patch length L, width W, input impedance Z_A , QWT length l_{qw} and width w_{qw} can be calculated using above mentioned formulas. Approximate values can also be obtained using online antenna calculators as given in [16]. For parameters $\epsilon_r = 2.2$, $h=1.575$ mm and $f_0 = 10\text{GHz}$, other parameters are calculated and given below.

$$\text{Free space wavelength } (\lambda) = \frac{c}{f_0} = 30\text{mm}; c = \text{speed of light in space} = 3 \times 10^8 \text{ m/sec}$$

$$\text{Patch length} = L = 9.0732 \text{ mm}$$

$$\text{Patch Width} = W = 11.8585 \text{ mm}$$

$$\text{Patch input impedance} = Z_A = 212.50\Omega \quad \text{using equation (2-12)}$$

$$\text{Characteristic impedance of QWT} = Z_0' = 103.07\Omega \quad \text{using equation (2-13)}$$

$$\text{QWT section length} = l_{qw} = 4.5886 \text{ mm}$$

$$\text{QWT section width} = w_{qw} = 1.4 \text{ mm}$$

$$\text{Width of } 50\Omega = w_{50} = 5.0687 \text{ mm}$$

$$\text{Length of } 50\Omega = l_{50} = 5.3583 \text{ mm}$$

Note that w_{50} , l_{50} , l_{qw} , w_{qw} are calculated by using LineCalc facility of ADS schematic feature and are optimized later in layout for desired results. Required parameters of LineCalc window are given in figure (2-8) for substrate RT Duroid 5880.

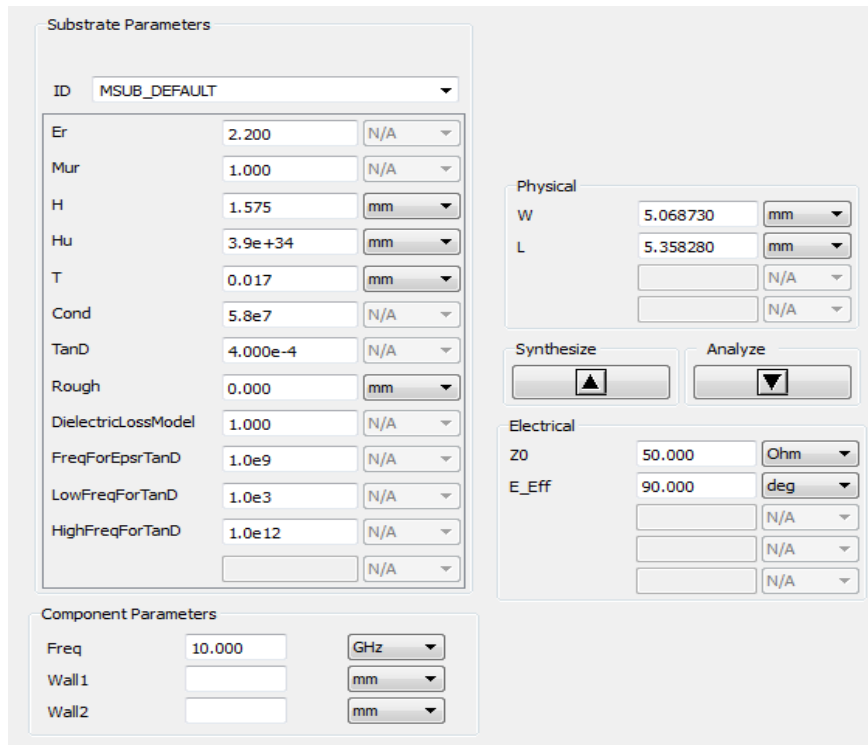


Figure 2-8: LineCalc parameters for RT Duroid 5880

After calculating all required parameters, 10 GHz microstrip patch antenna is designed in layout of ADS momentum software. Its design is given in following figure (2-9). Note that, it is required to define the substrate parameters in the layout. After carefully designing the patch antenna, it was simulated and S-parameters, antenna parameters, 3D radiation pattern and 2D gain & radiated power plots were analyzed and are given in figures (2-10, 2-11, 2-12 and 2-13), respectively. Return loss of -29.95dB is observed at desired frequency of operation 10GHz. While efficiency of antenna obtained as 85.26% with 6.730 dB gain and 7.399 dB directivity.

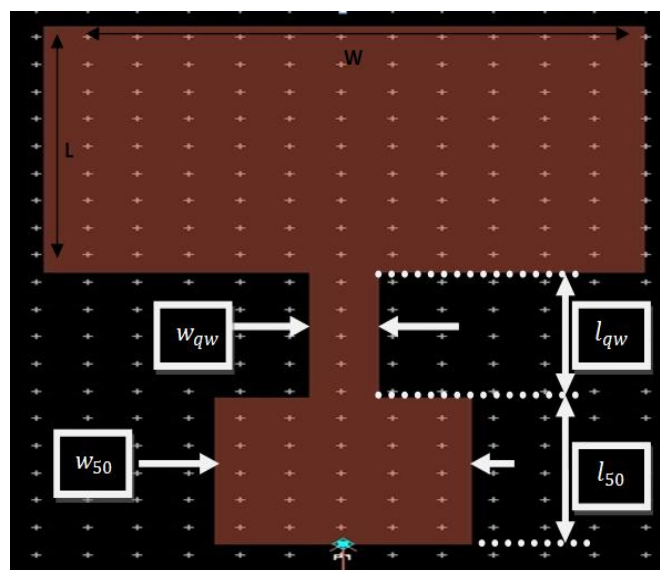


Figure 2-9: Layout design of 10 GHz patch antenna

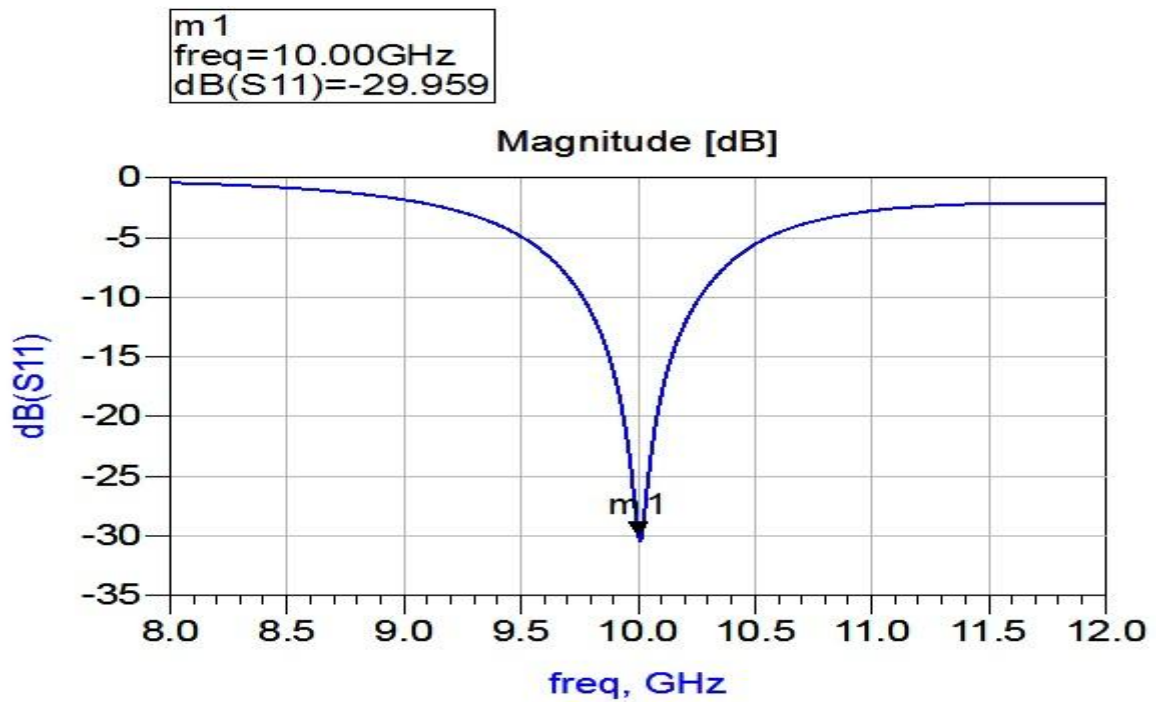


Figure 2-10: S11 of designed 10GHz patch antenna

| Antenna Parameters | | |
|-------------------------------------|-------------|----------|
| Power radiated (Watts) | 0.00214099 | |
| Effective angle (Steradians) | 2.28716 | |
| Directivity(dBi) | 7.39914 | |
| Gain (dBi) | 6.7302 | |
| Maximim intensity (Watts/Steradian) | 0.000936092 | |
| Angle of U Max (theta, phi) | 23 | 270 |
| E(theta) max (mag,phase) | 0.839825 | 39.8184 |
| E(phi) max (mag,phase) | 0.0012906 | 91.7899 |
| E(x) max (mag,phase) | 0.0012906 | 91.7899 |
| E(y) max (mag,phase) | 0.773063 | -140.182 |
| E(z) max (mag,phase) | 0.328146 | -140.182 |

Figure 2-11: Antenna parameters of designed 10GHz patch antenna

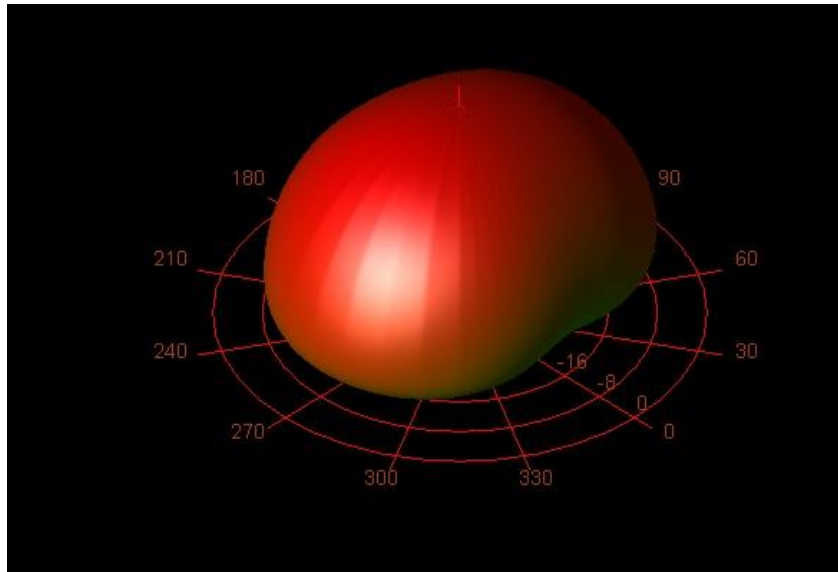


Figure 2-12: 3D radiation pattern of designed 10GHz patch antenna

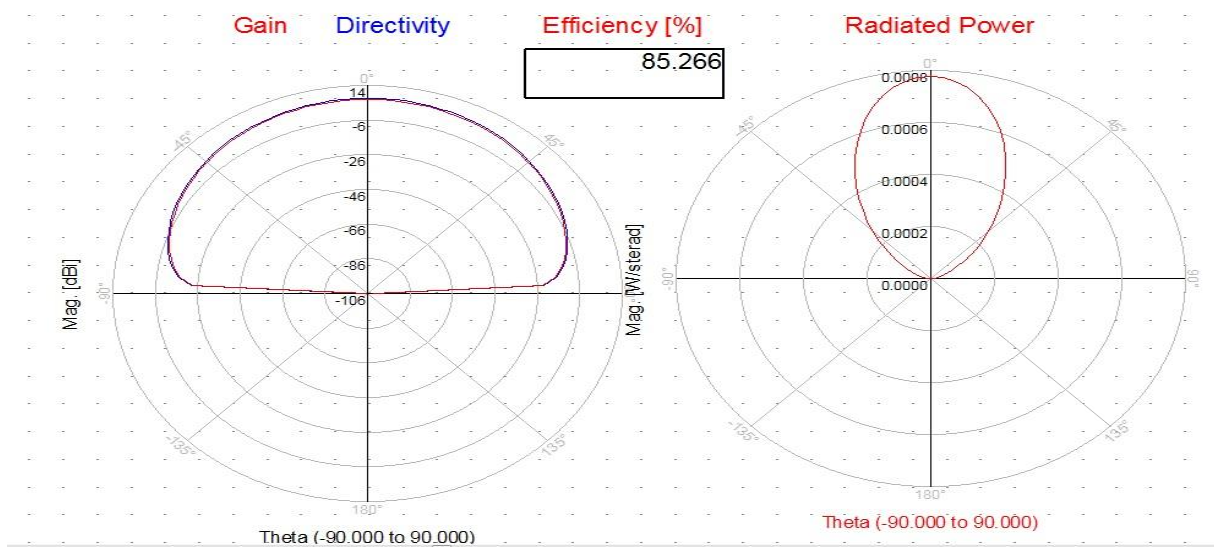


Figure 2-13: 2D gain and radiated power plots of designed 10GHz patch antenna

2.3.5 Microstrip Antenna Array

By increasing the transmit power, the coverage and operation range of a passive system can be increased; however it is not applicable due to regulations on transmitting power. In this case, keeping the same transmit power, operation range of the communication channel can be raised by thanks of antenna array configuration. An antenna array often called ‘phased array’ consists of set of two or more than two antenna elements. Purpose is that the signals from the antennas are combined or

processed in order to achieve improved performance over single antenna performance [17]. Antenna array can be used to increase the gain of overall system, to provide diversity reception, to focus the reception of signals from any particular direction as DOA system and cancel out interference from a particular set of directions, to estimate the direction of arrival of received signals; and to maximize the Signal to Interference plus Noise ratio (SINR) [18].

As mentioned in [7], due to the advantage offered by the arrays of the microstrip antennas, feed network as well as the radiating elements can be printed on the same single layer on printed circuit board (PCB) of different types of material substrates. Full integration (antenna elements, feeding circuitry and the chips) is possible with technology. Microstrip antennas are used in many possible array configurations in order to increase the gain. Patch arrays are popular for fixed-beam applications (radiating network and the feed network on the same substrate) for low cost lithographic PCB techniques. Inter element spacing is less than one wavelength to avoid grating lobes and greater than half wavelength to provide room for feed lines (to achieve higher gain for a given number of elements and to reduce mutual coupling). Mutual coupling effects are not significant for patches that are spaced 0.57λ . Array can be linear, planar or conformal; the feed can be parallel, series or hybrid. As an example of 4 elements array, figure 2-14 is shown. The overall antenna pattern of a microstrip patch array is formed with the contribution of each element. Antenna pattern can be obtained by multiplying the single element pattern with a parameter called Array Factor (AF). With angle differences, AF varies and shapes the single element pattern to form the overall pattern of array. AF depends on the distances between patch elements, total number of patch elements, the phase and amplitude differences of the currents between adjacent patch elements and the frequency of the field. As stated in [19] and [20], cross-polarization generated by higher order modes of a patch antenna can be cancelled by proper use of the symmetry, elements placed symmetrically with given element spacing in x and y coordination system.

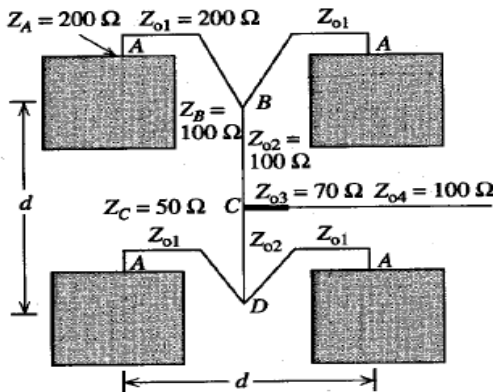


Figure 2-14: 4-element patch array [7].

If we have M elements in x-axis with element spacing d_x and N elements in y-axis with element spacing d_y , phase shift of β_x between the elements in x-axis and β_y between elements in y-axis; and element excitation as I_m in the x-axis and I_n in the y-axis, then array factor of the planar antenna array can be calculated as in equation (2-19) [20].

$$AF = \sum_{m=1}^M I_{m1} e^{j(m-1)(kd_x \sin\theta \cos\phi + \beta_x)} X \sum_{n=1}^N e^{j(n-1)(kd_y \sin\theta \sin\phi + \beta_y)} \quad (2-19)$$

In this thesis work, in order to take the sum and difference of two signals, an array of two elements is designed with element spacing of 0.6λ . This is more described in details in section (4).

3. Rat Race Coupler

Rat race coupler or hybrid ring coupler having four ports is a type of coupler mainly used in RF/microwave systems. It provides a great advantage of being easy to realize in planar technologies such as microstrip and striplines although waveguide rat race couplers also exist in practical. Power dividers and couplers are fundamental and important passive circuits in RF/microwave front end. They can be incorporated with balanced mixers and balanced amplifiers for equal or unequal power division [21].

Typical design of rat race ring coupler is shown in figure 3-1 which consists of two input ports, named as port 1 and port 2 and two output ports, named as port 3 (sum) and port 4 (difference). Therefore, this type of coupler is used to provide the sum and difference of two in phase input fed signals. Each port of top half ring is spaced from each other by $\lambda/4$ distance while bottom ring is $3\lambda/4$ in length. The ring has a characteristic impedance of factor $\sqrt{2}$ compared to port impedance, for example, for 50Ω , it is $\sqrt{2} * 50 = 70.7 \Omega$. Its circumference is 1.5λ or 6 times $\lambda/4$. So radius of ring can be obtained from $S = 2\pi r$ where S is circumference ($6 * \lambda/4$) and r is radius. For an ideal 3dB rat race coupler, full s-parameter (scattering) matrix is given as in this matrix

$$S = \frac{-j}{\sqrt{2}} \begin{pmatrix} 0 & 1 & 0 & -1 \\ 1 & 0 & 1 & 0 \\ 0 & 1 & 0 & 1 \\ -1 & 0 & 1 & 0 \end{pmatrix} \quad (2-21)$$

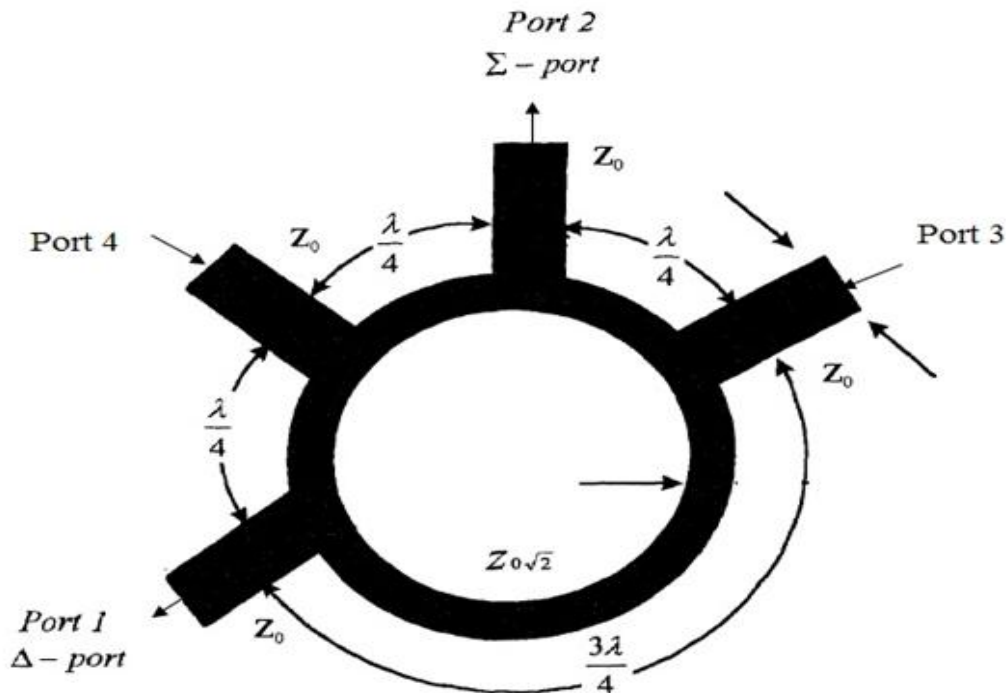


Figure 3-1: Typical rat race ring coupler design

3.1 180° Hybrid Rat Race Ring Coupler

As mentioned earlier, 180° hybrid ring couplers are four-port devices used to either equally split an input signal or to sum two combined signals. An additional benefit of the hybrid ring is to alternately provide equally-split but 180 degree phase-shifted output signals. This configuration creates a lossless device with low VSWR, excellent phase & amplitude balance, high output isolation and match output impedances.

The parameters, substrate thickness h and dielectric constant ϵ_r are noticeable in design because they relate to the characteristic impedance Z_0 , and should be calculated carefully [22]. In this work h and ϵ_r , are chosen as 1.575 mm and 2.2 respectively. The ring of coupler consists of six sections, the length of each section equals to L , (where $L=\lambda/4$) and by using the following expression we can calculate the radius r , of the ring [22].

$$r = \frac{360 L}{2\pi C} \quad (2-21)$$

Where C , is the angle in degree [23][24], this mean C , equal 60° for each section.

For this thesis work, 180° hybrid ring coupler has been designed in order to obtain the difference and sum patterns of the received signals. For this purpose first using ADS schematic tool, a 180° hybrid rat race ring coupler has been designed for desired frequency of 10 GHz. Its schematic design with all calculated parameters is given in figure 3-2. Schematic simulation results showed better S-parameters for all 4 ports of coupler. In order to understand in easy way, let's assign the names to each port. Port 1 is the difference port, port 2 is the sum port, and Port 3 and Port 4 are the input feeding ports. Return loss of each port (S_{11} , S_{22} , S_{33} , S_{44}) is given in figure 3-3 which shows nice matching of each port with return loss of -45.94 dB. Port isolation between each port is shown in figure 3-4. Figure 3-5 shows the phase difference of 180° in order to obtain the difference of two received signals. Figure 3-6 shows two input signals (port 3 and 4) arriving in phase at sum port (port 2).

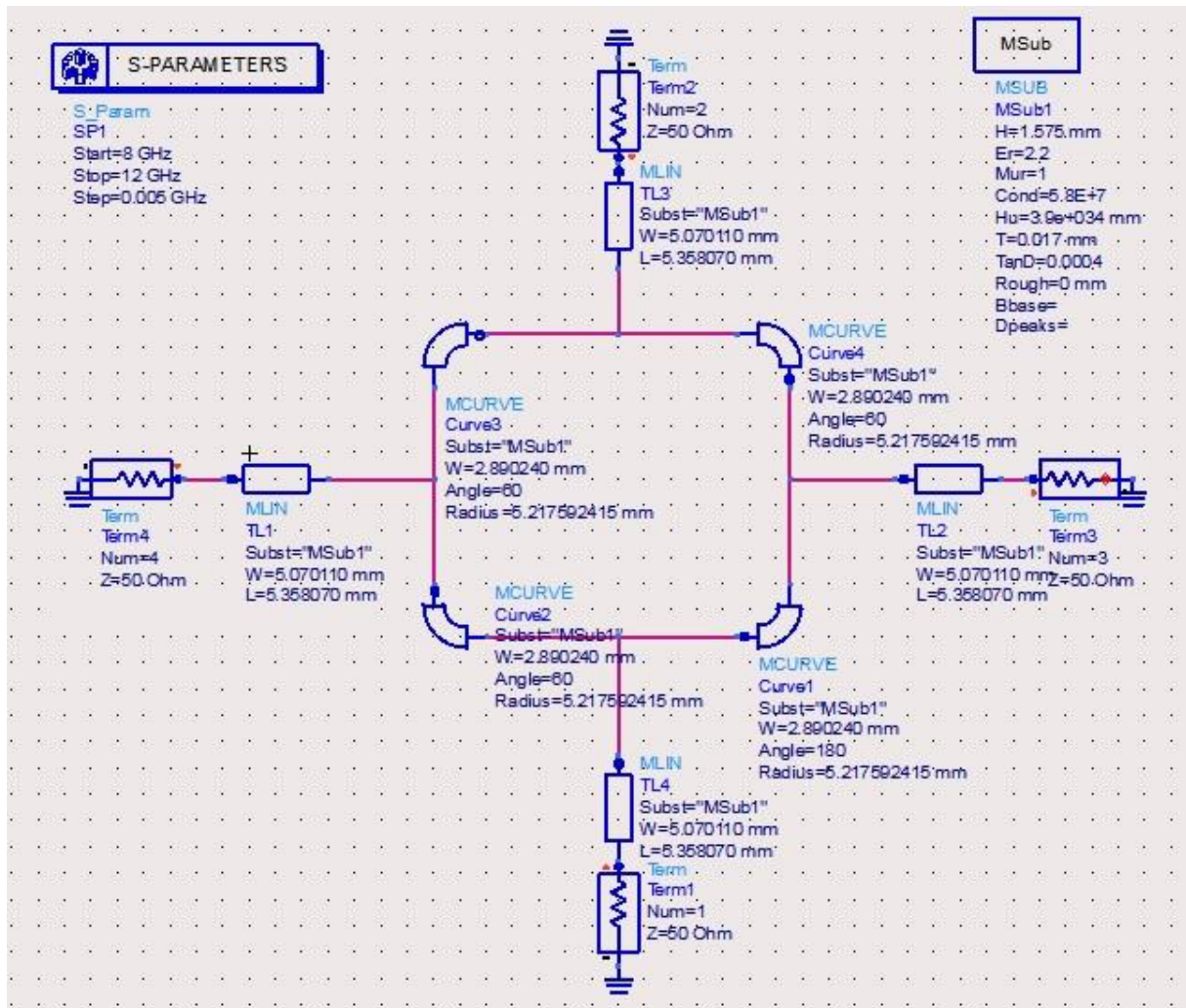


Figure 3-2: Schematic design of 180° hybrid rat race ring coupler

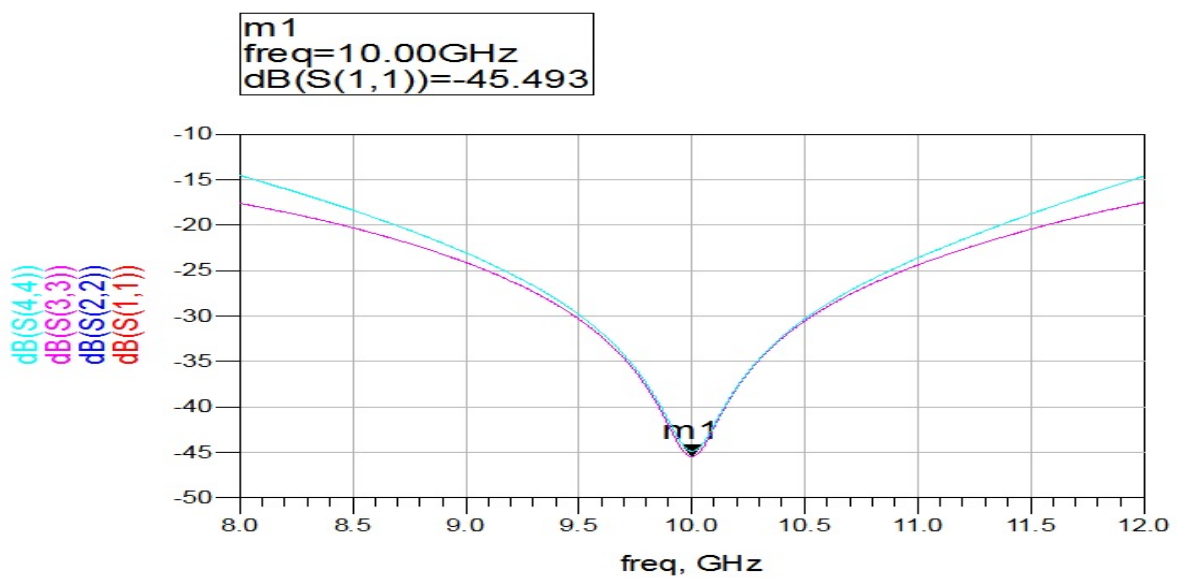


Figure 3-3: Schematic S11, S22, S33 and S44 of port1, port2, port3 and port4, respectively.

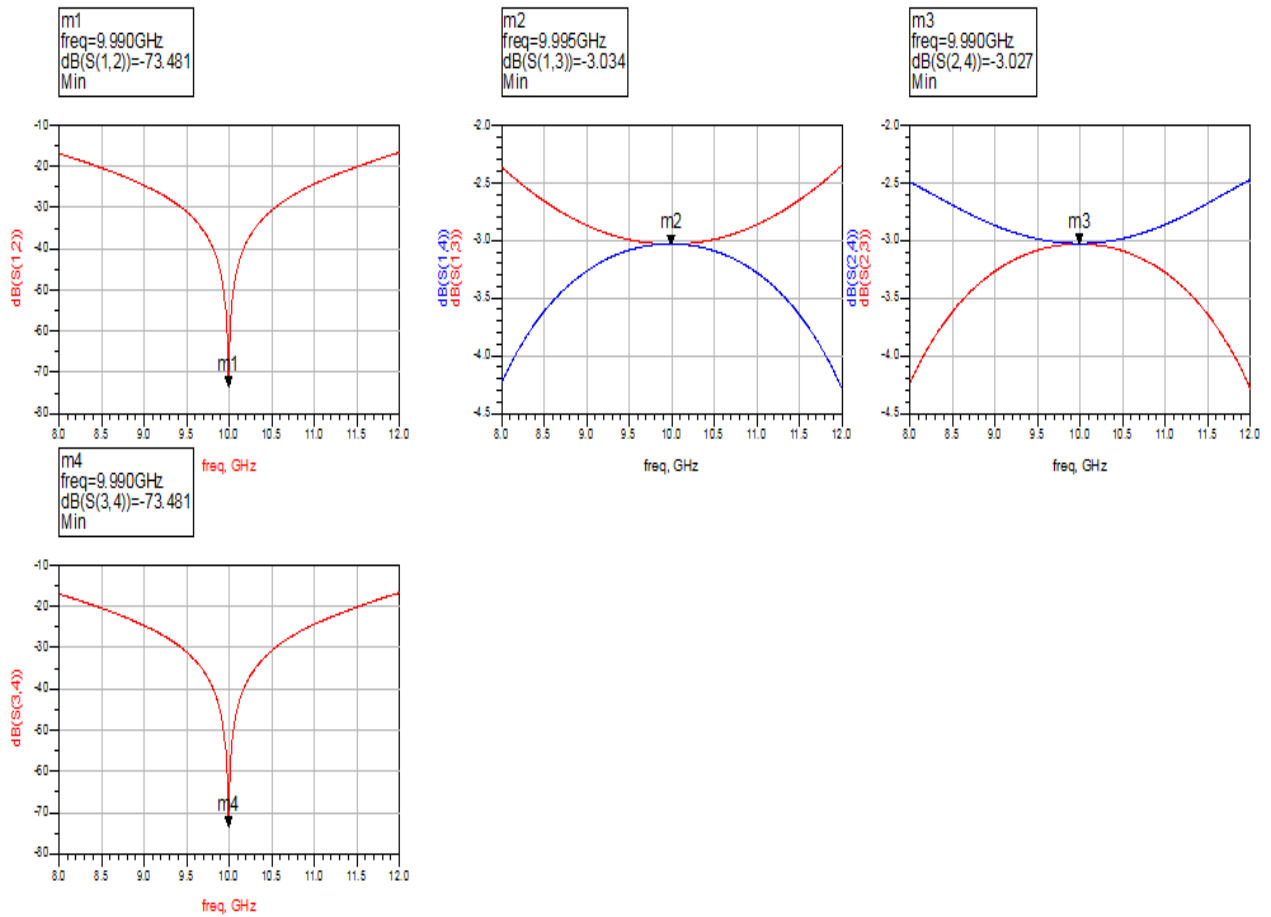


Figure 3-4: Port isolations

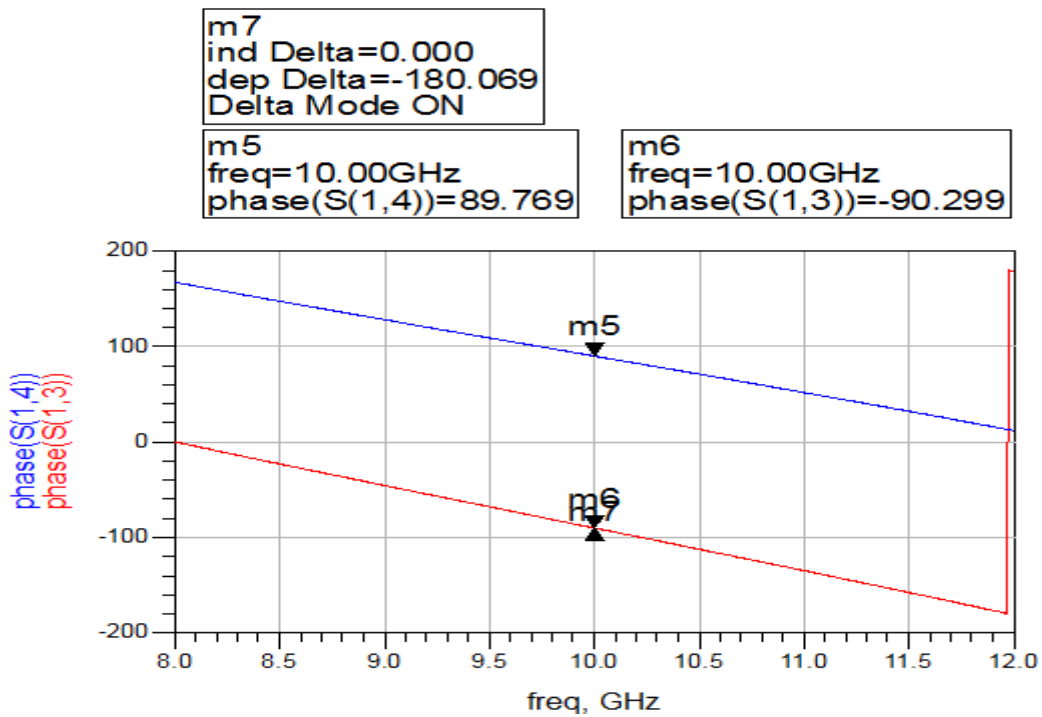


Figure 3-5: Phase difference of 180° in between two input signals at ports 3 and 4

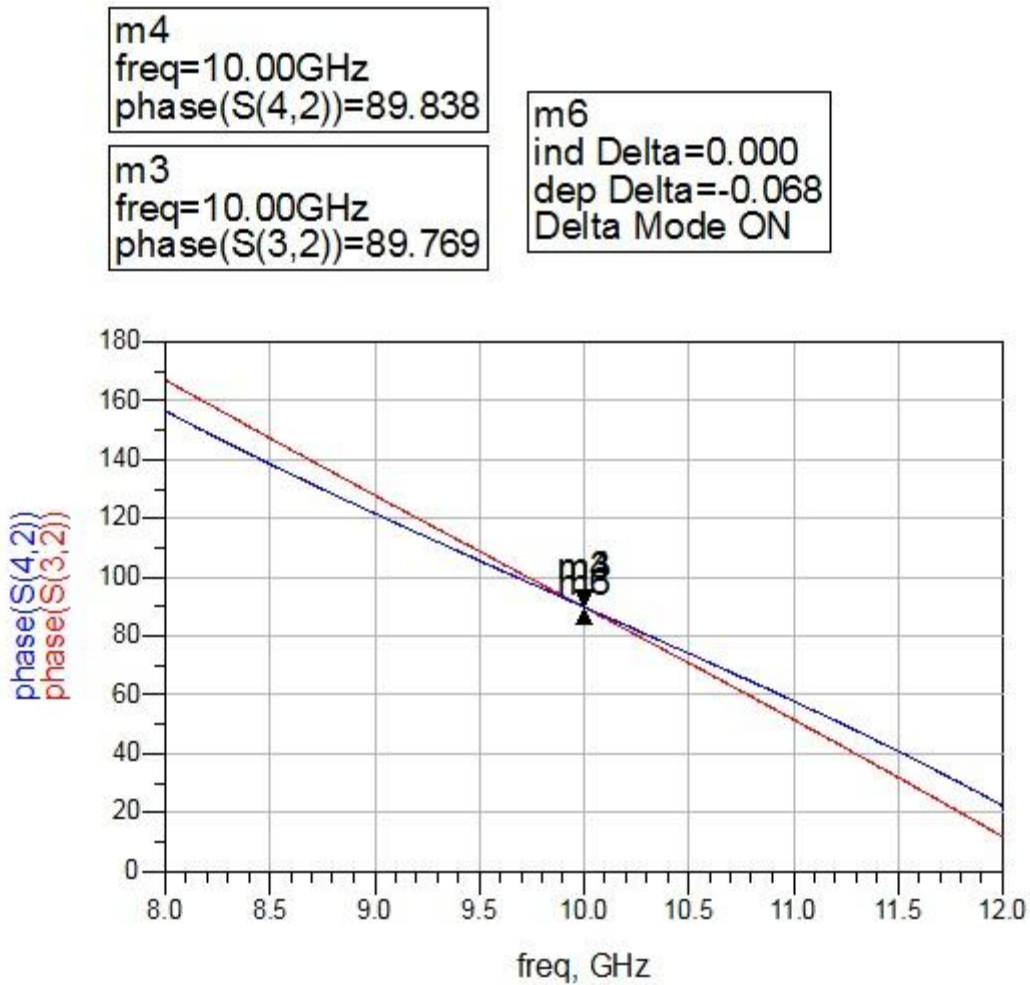


Figure 3-6: Two input signals arriving in phase at sum port

Later schematic design has been imported in layout tool of ADS and its design is given in figure 3-7. After tuning/optimizing the layout design, simulation was run and S-parameters are observed. This time S-parameters are slightly changed than schematic because in layout simulations, ADS performs in chunks by making mesh around the design. Return loss of each port is given in figure 3-8. Port isolation between each port is shown in figure 3-9. Figure 3-10 shows the phase difference of 180° in order to obtain the difference of two received signals. Figure 3-11 shows Two input signals (port 3 and 4) arriving in phase at sum port (port 2).

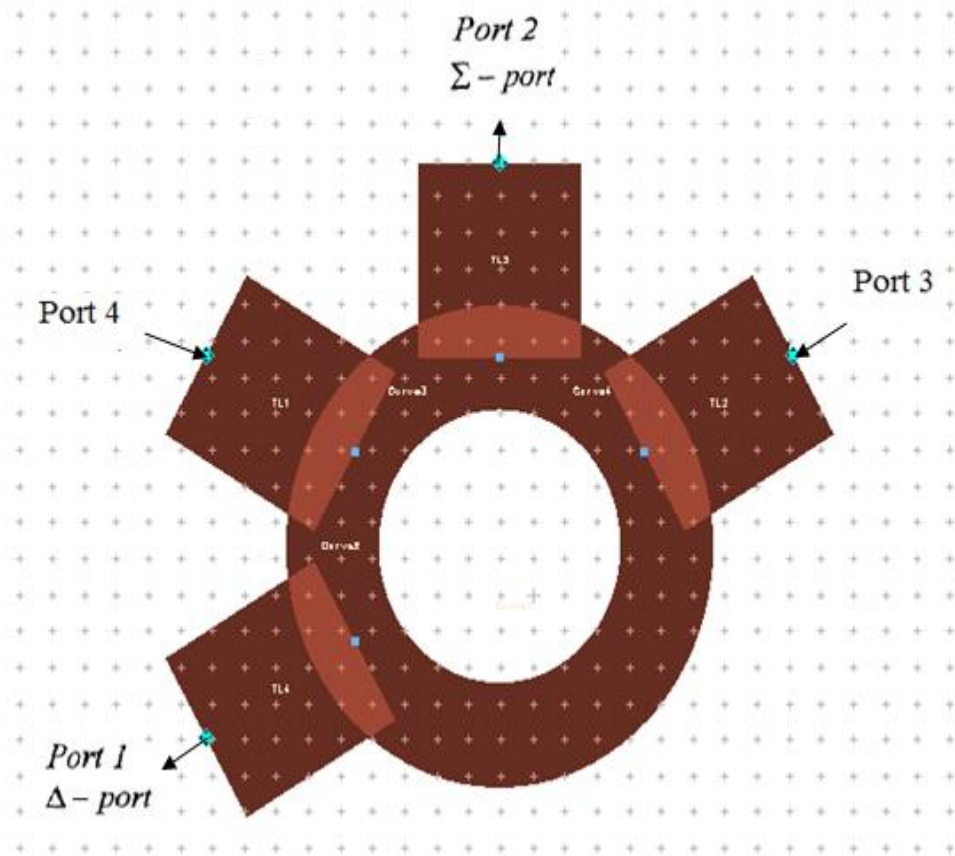


Figure 3-7: Layout design of rat race coupler at 10 GHz central frequency

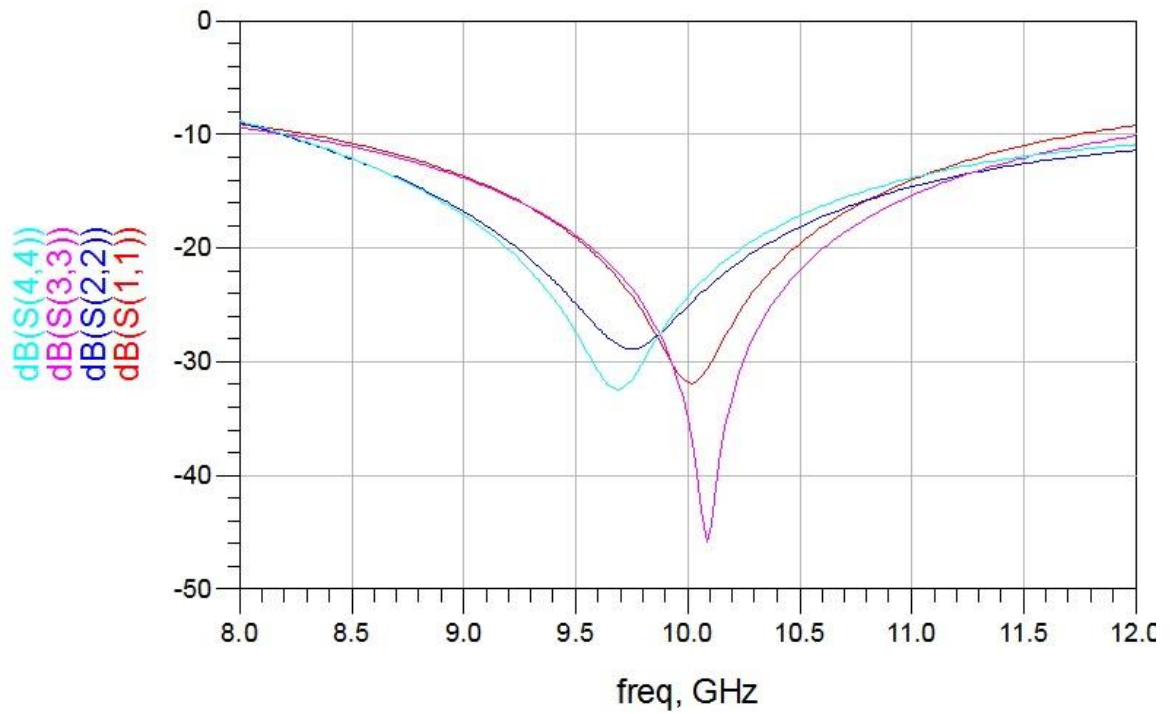


Figure 3-8: Layout S11, S22, S33 and S44 of port1, port2, port3 and port4, respectively

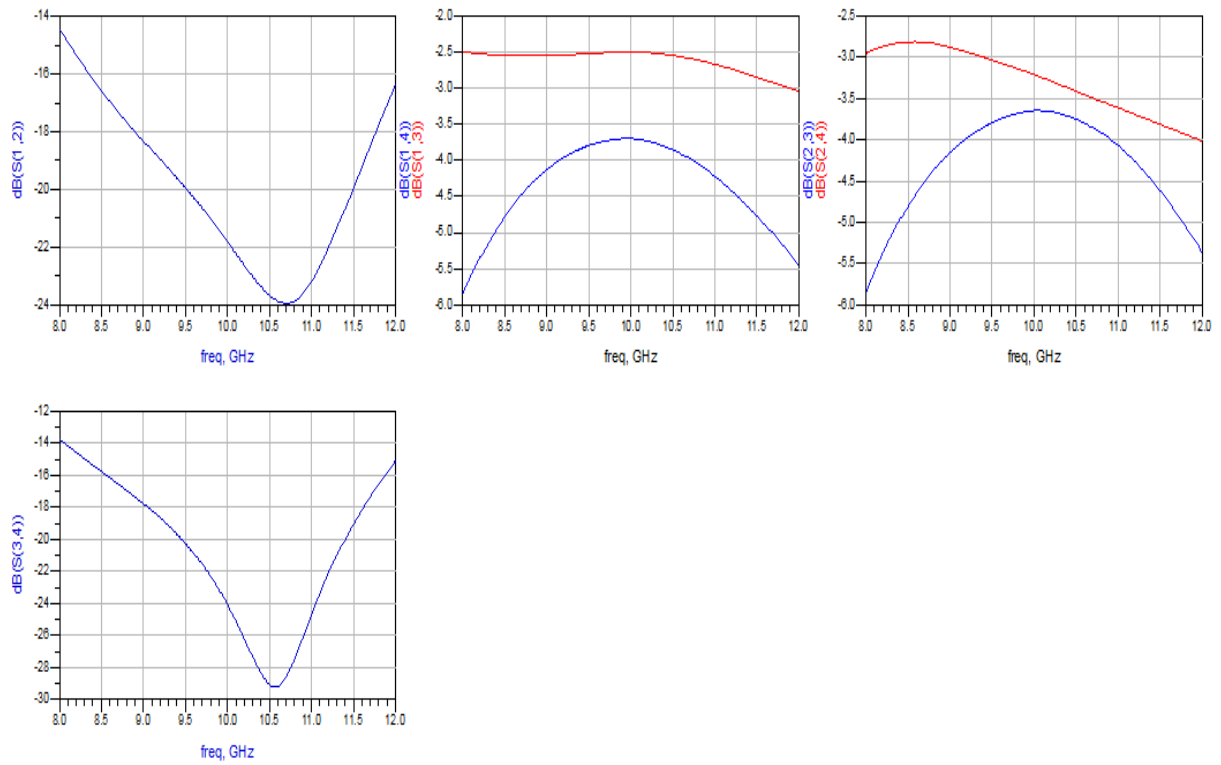


Figure 3-9: Port isolations

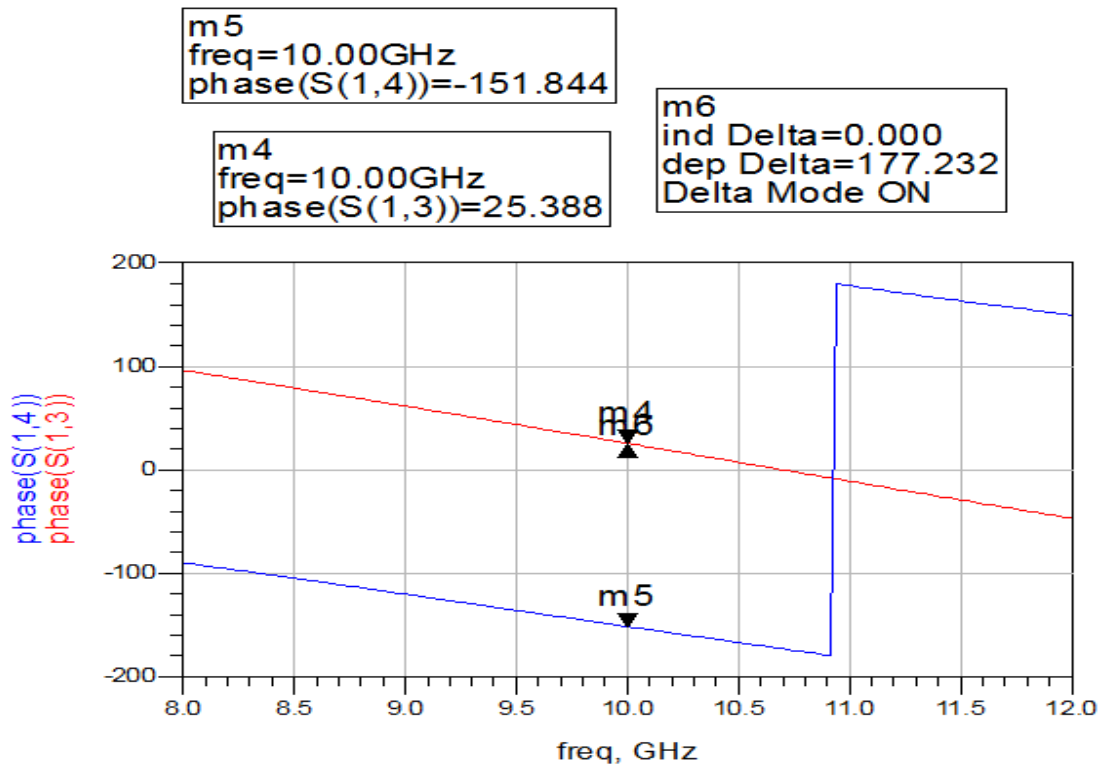


Figure 3-10: Phase difference of 180° in between two input signals at ports 3 and 4

m2
freq=10.00GHz
phase(S(2,3))=-127.068

m1
freq=10.00GHz
phase(S(2,4))=-123.517

m3
ind Delta=0.000
dep Delta=-3.551
Delta Mode ON

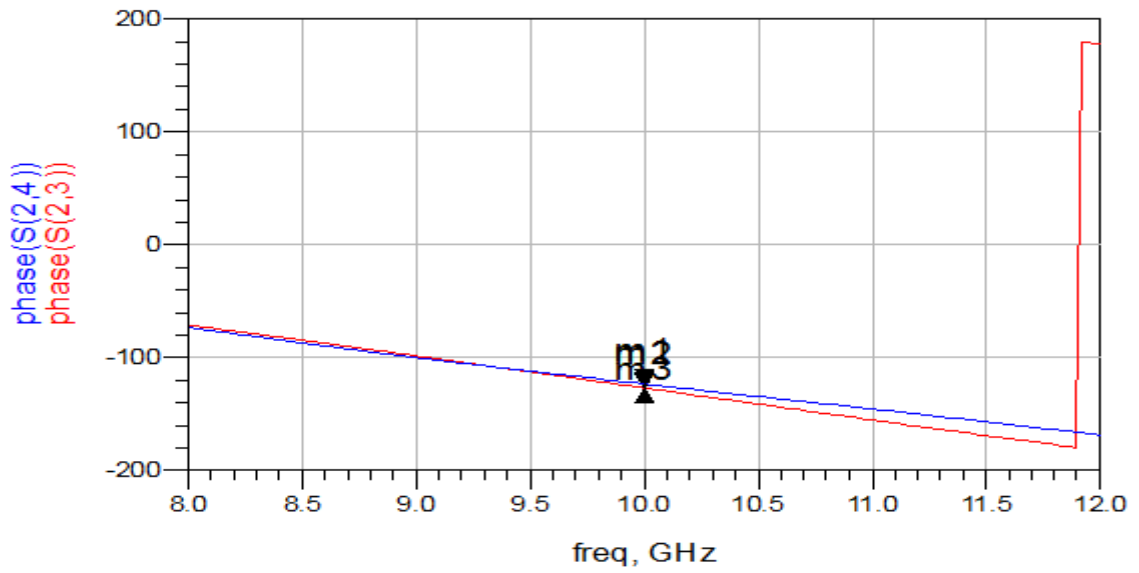


Figure 3-11: Two input signals arriving in phase at sum port

4. DOA Finding System Design and Experimental Results

As discussed earlier, the objective of this thesis is to design a microstrip patch antenna array with rat race coupler in x-band of frequency to estimate the direction of arrival (DOA) or the angle of arrival (AOA) of received signals using the difference and sum patterns of the coupler. After studying and successfully implementing patch antenna and rat race coupler individually, its now time to integrate all these parts according to mentioned design to analyze the difference and sum patterns in order to find out the AOA in both axis separately. This analysis is discussed step by step in following sections through Matlab coding, ADS simulations and practically fabrications of desired circuits.

4.1 $\Delta - \Sigma$ Pattern Analysis through Matlab coding

Difference and sum pattern equations are given in equations (2-1 and 2-2) from which it is possible to obtain the AOA by using equation (2-3). In order to analyze the Δ and Σ pattern numerically through Matlab, it is required to have the radiation pattern of antenna element. For this purpose, radiation pattern of single patch antenna already simulated in ADS can be used in order to plot the difference and sum patterns. By multiplying the 2D gain pattern values of single patch antenna with equations (2-1 and 2-2), difference and sum plots are obtained through Matlab coding. Note that, this Matlab coding is given in appendix A. After running the code, obtained normalized difference and sum pattern v.s angle θ (in degrees) plot is given in figure 4-1.

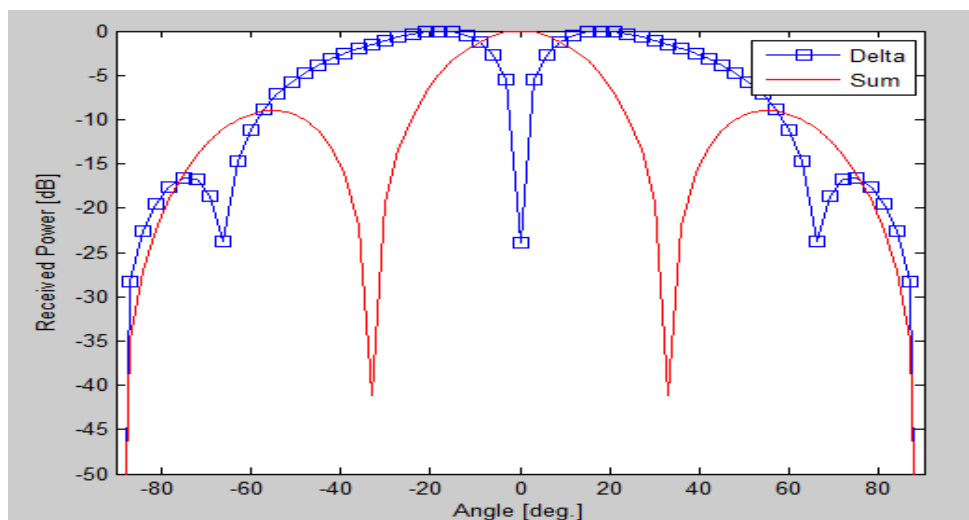


Figure 4-1: Numerically obtained Δ and Σ patterns

4.2 Estimating DOA in θ axis

Estimating the direction of received signal specially in x-band of frequency is a challenging task for radar, military and communication system applications. As mentioned earlier that it is necessary to focus the reception in estimated direction and rejecting in all other directions, which in result increases the quality of received signals. For this purpose, there exist many algorithms in finding the DOA but these algorithms are generally complex [4]. Due to one to one relationship between direction of a signal and the associated received steering vector [5], it is therefore possible to estimate the direction of received signal by inverting this relationship. In this thesis work a novel antenna array system using difference (Δ) and sum (Σ) patterns of received 10 GHz signal is proposed. This proposed DOA finding system consists of microstrip patch antenna array, rat race ring coupler and feeding network.

Here, in order to take the two sample signals, array of two patch antennas has been implemented. Spacing between two elements is chosen as 0.6λ (18mm) because more than one λ spacing create grating lobes while less than 0.5λ produce mutual coupling between two elements patterns which in result decrease signal to interference/noise ratio of the received signal. After receiving the signal from each antenna element, signals are fed as two input signals to the 4 ports 180° hybrid rat race ring coupler. Coupler by performing its operation according to equations (2-1 and 2-2), generates difference and sum patterns of fed input signals at two output ports, called as Δ and Σ ports. This setup of array antennas and coupler in vertical direction is shown in figure 4-2 which is simulated in ADS momentum software's layout tool. After designing the setup, S-parameters, far field patterns and antenna parameters of Δ and Σ are analyzed and are given in figures 4-3, 4-4, 4-5, respectively. By using Δ and Σ pattern equations and values of θ from 0 to 30 degrees, absolute amplitude values and phases have been calculated as given in table 4-1. As shown in figure 4-4, in ADS far field simulation, using these table values, Δ and Σ ports were excited and beam was observed to be moved from 0 to 30 degrees as values of θ varies from 0 to 30 degrees ($\phi=90^\circ$), respectively, with approximately $\pm 3^\circ$ error at some θ values. As shown in figure 4-5, maximum gain obtained is 9.47dBi and directivity 10.99 dBi.

Table 4-1: Calculated absolute amplitude and phase of Δ and Σ from equations (2-1 and 2-2).

| θ [deg.] | Σ Amplitude | Σ Phase | Δ Amplitude | Δ Phase |
|-----------------|--------------------|----------------|--------------------|----------------|
| 0 | 2 | 0 | 0 | 0 |
| -15 | 1.667 | -27.95 | 0.9375 | 62.04 |
| 15 | 1.667 | 27.95 | 0.9375 | -62.04 |
| -30 | 1.1756 | -54 | 1.618 | 36 |
| 30 | 1.1756 | 54 | 1.618 | -36 |

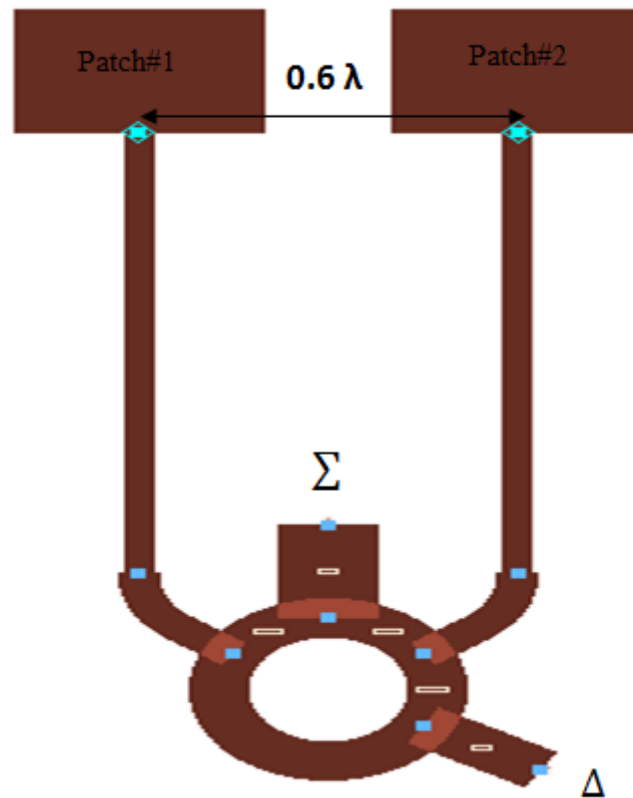


Figure 4-2: ADS layout design of Δ - Σ Pattern, circuit 1 (theta axis) .

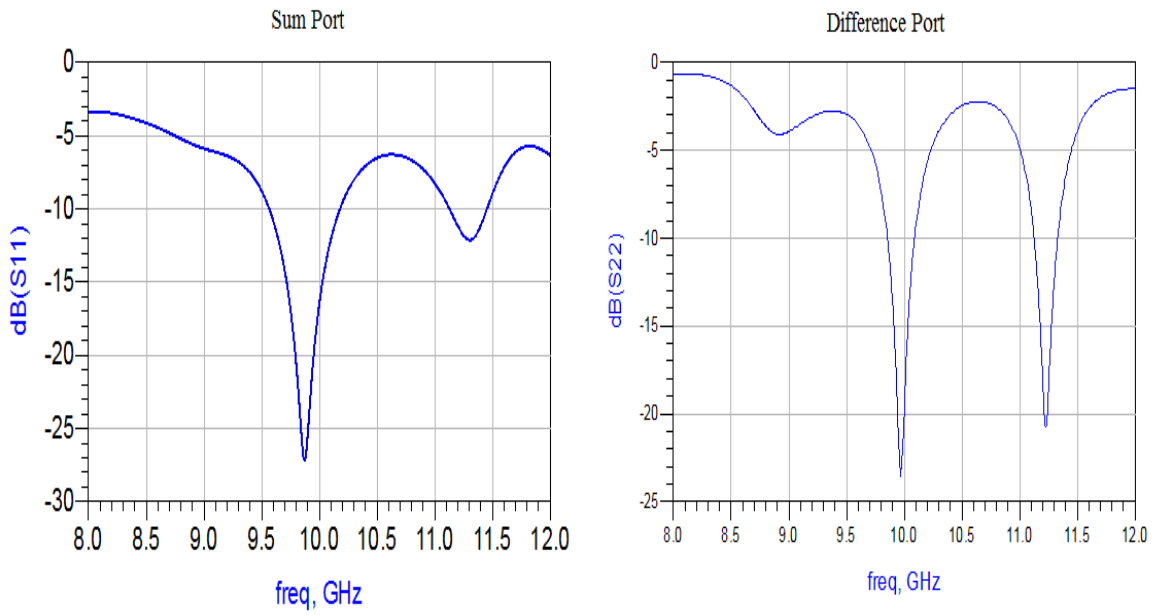
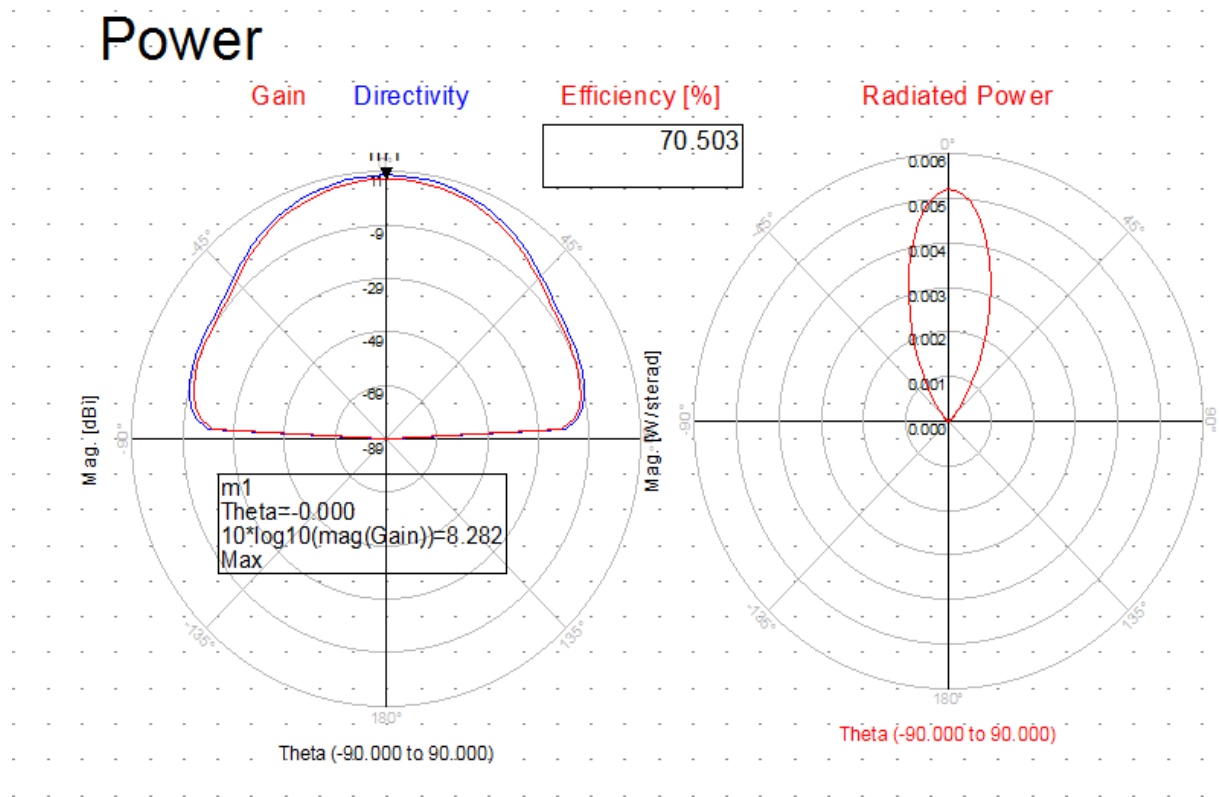
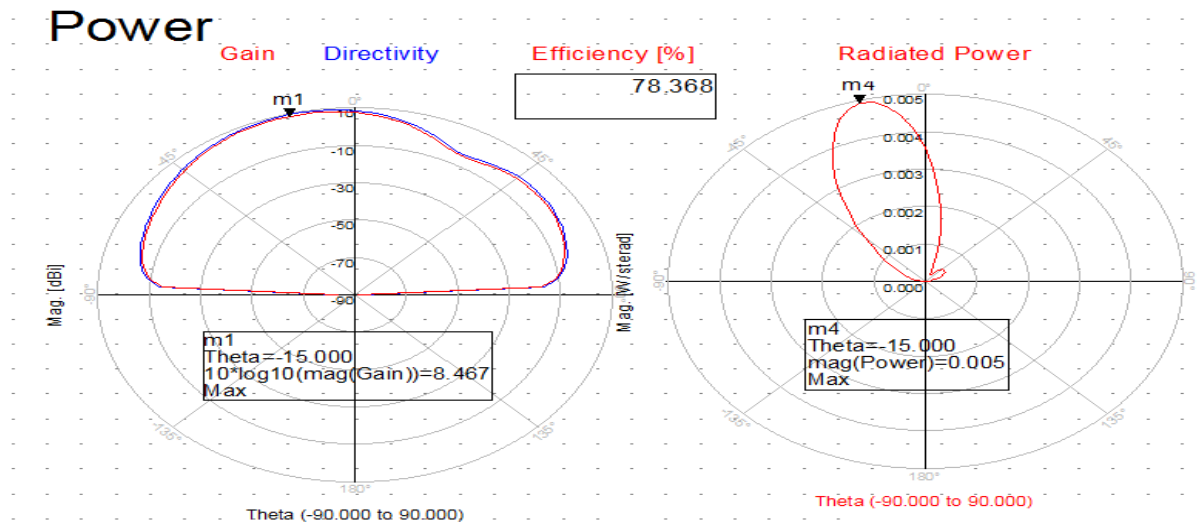


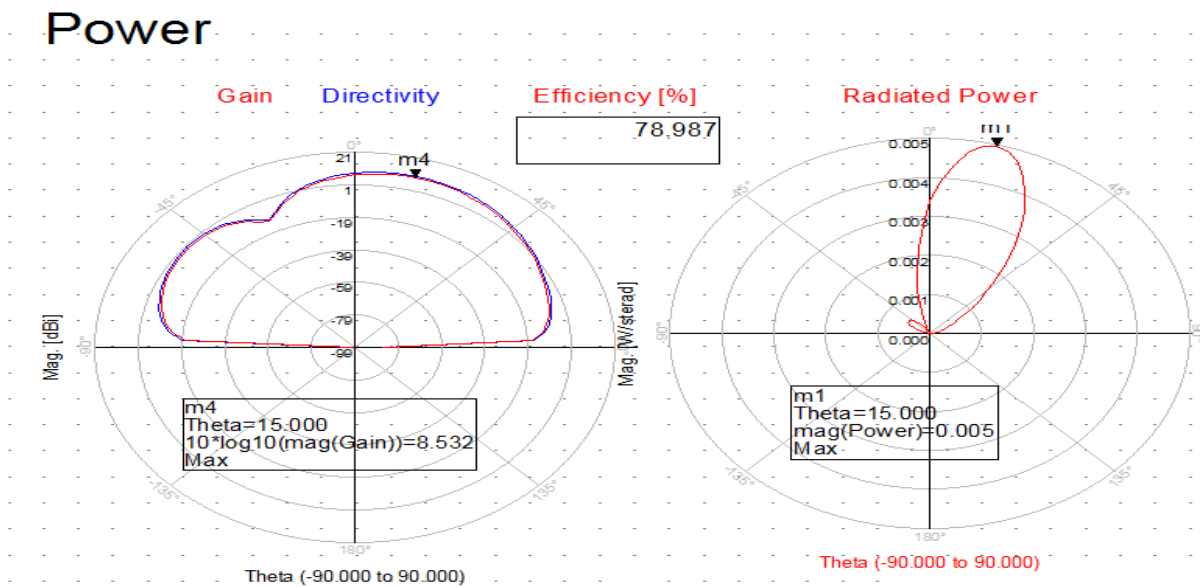
Figure 4-3: S-parameters of Δ and Σ ports, simulated in ADS layout



a) 2D gain and Radiated Power plots at $\theta=0^\circ$



b) 2D gain and Radiated Power plots at $\theta = -15^\circ$



c) 2D gain and Radiated Power plots at $\theta = +15^\circ$

Figure 4-4: Far field patterns at different applied theta values.

| Antenna Parameters | |
|------------------------------|------------|
| Power radiated (Watts) | 0.00683596 |
| Effective angle (Steradians) | 0.999609 |
| Directivity(dBi) | 10.9938 |
| Gain (dBi) | 9.47585 |

Figure 4-5: Antenna parameters

Simulated ADS layout design has been fabricated for experimental results to find out the DOA in theta axis. Let's call this design as circuit1. From ADS layout, gerber file was exported in order to fabricate the design on selected RT Duroid 5880 material ($\epsilon_r = 2.2$, *thickness* = 1.575mm). Exported file was given to PCB designing machine for etching. This fabricated circuit is shown in figure 4-6 with SMA connectors soldered from back side. Later this circuit was tested in Anechoic Chamber of Sabanci University, SUNUM department for measured results. In this regard, a horn antenna was used as a transmitting antenna and constructed circuit used as receiving of 10GHz signal from transmitting horn antenna. This setup is shown in figure 4-7. Further, using Agilent Network Analyzer (up-to 50GHz), S-parameters and Δ & Σ patterns have been measured which later plotted by importing in Matlab and are shown in figures 4-8 and 4-9 respectively. Having Δ and Σ patterns of experimental setup, angle of arrival in θ -axis can be estimated. For this purpose a Matlab code is written in which, measured Δ and Σ patterns are imported and used in following equation (4-1) then by using AOA equation, angle of arrival has been found, from -40 to +40 degrees as expected with some minor rms error of less than 5 degrees. These estimated values of angle of arrival of received signal v.s actual transmitted signal angles are plotted in Matlab from 0 to 40 degrees and are shown in figure 4-10. Note that written Matlab code for this work is given in appendix B.

$$E_x = E_\theta \cos\theta \cos\phi - E_\phi \sin\theta \quad (4-1)$$

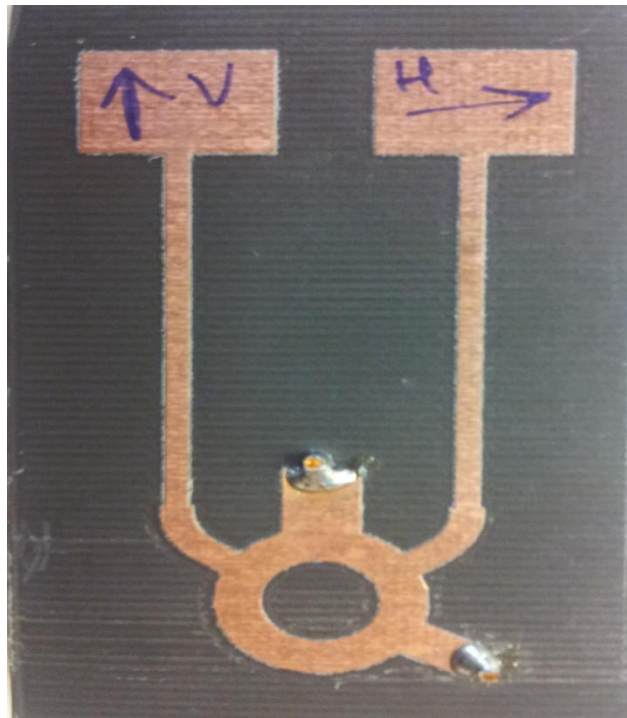


Figure 4-6: Difference – Sum Pattern circuit 1 fabricated (theta axis)

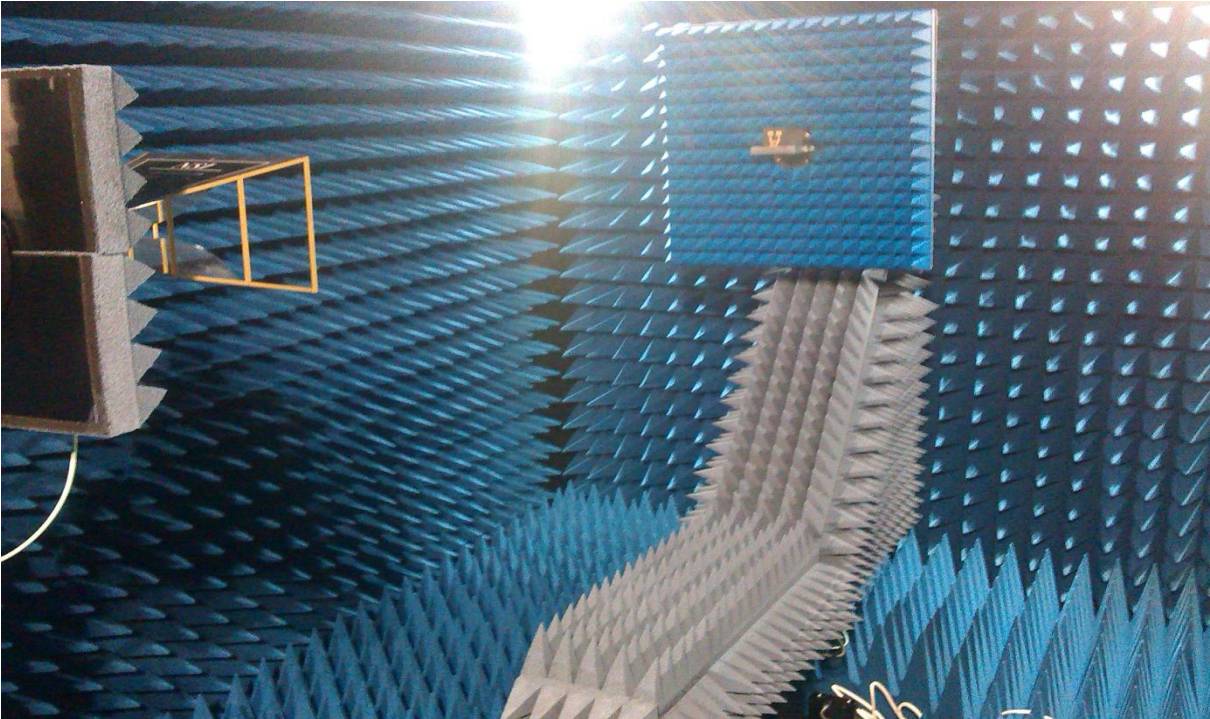


Figure 4-7: Testing the circuit in Anechoic chamber with Horn transmitting antenna and fabricated circuit as receiving

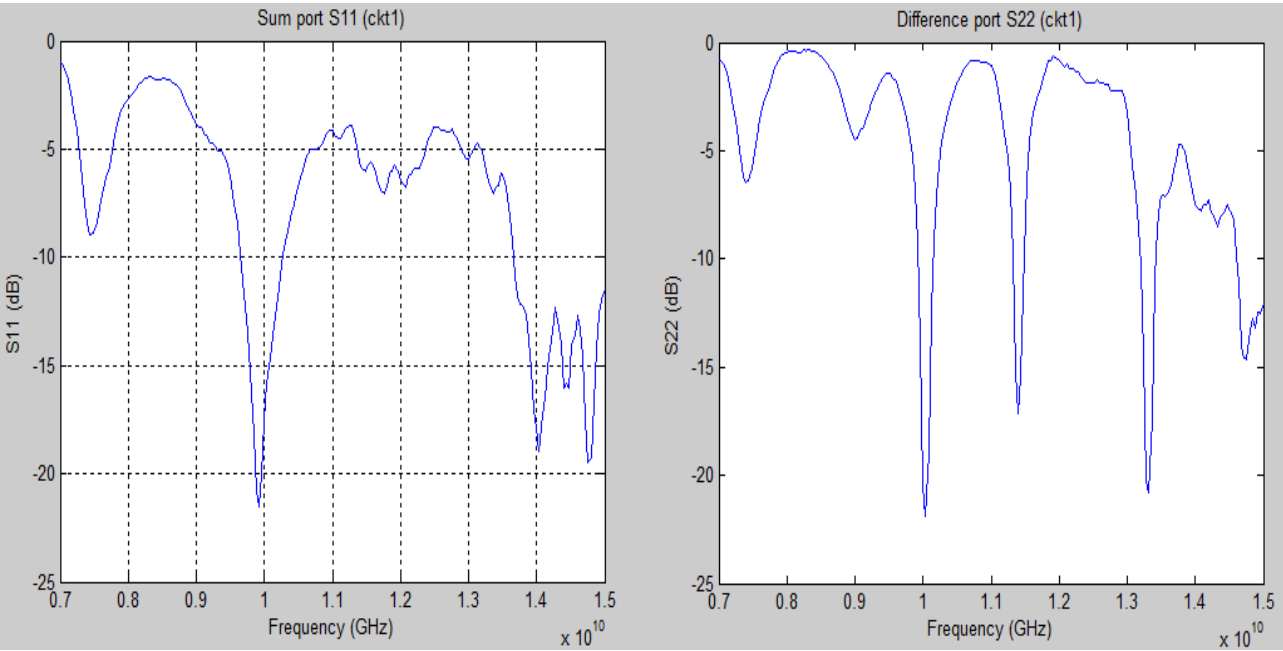


Figure 4-8: Measured S-parameters of Σ and Δ ports, respectively

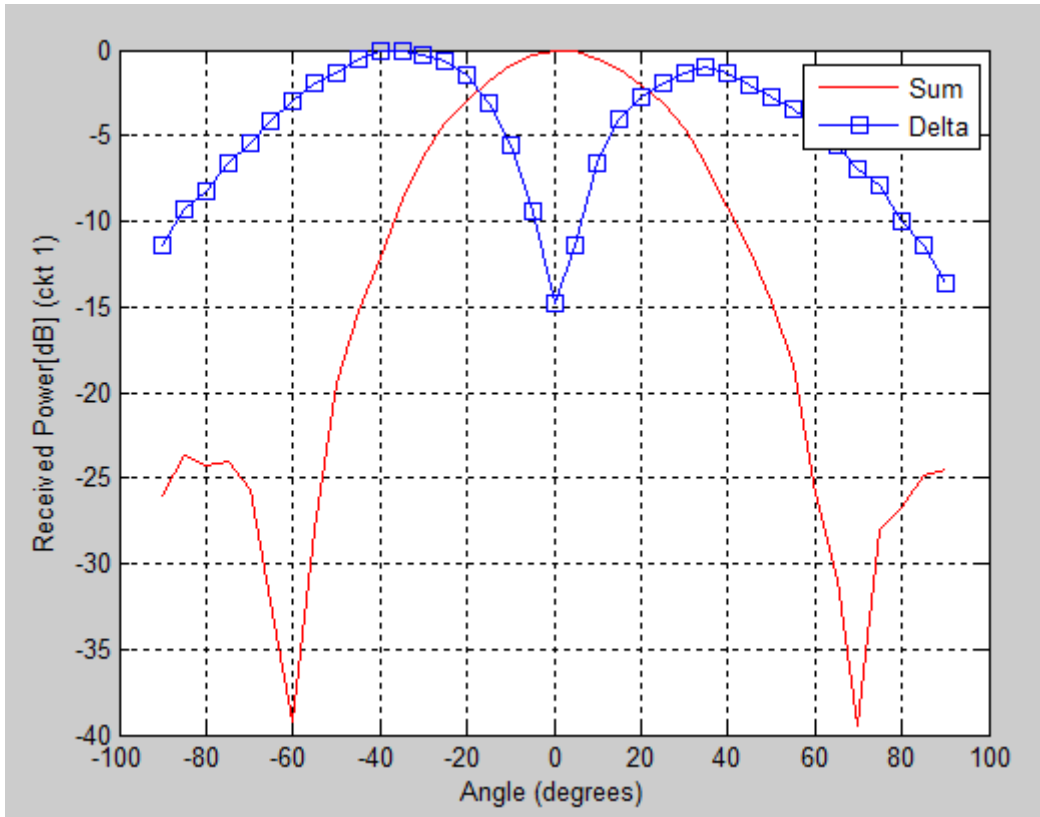


Figure 4-9: Measured normalized Δ and Σ patterns of circuit 1

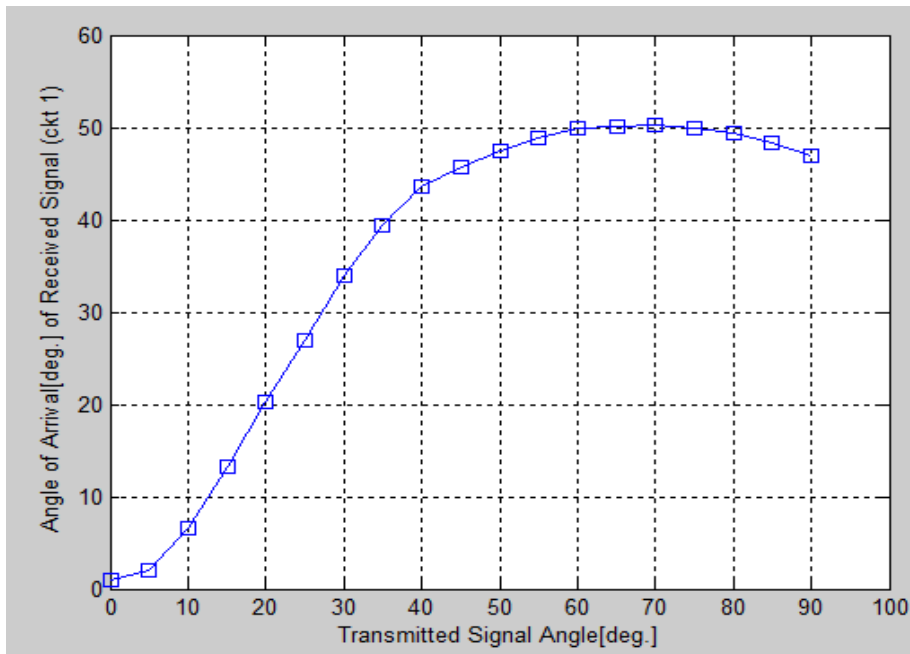
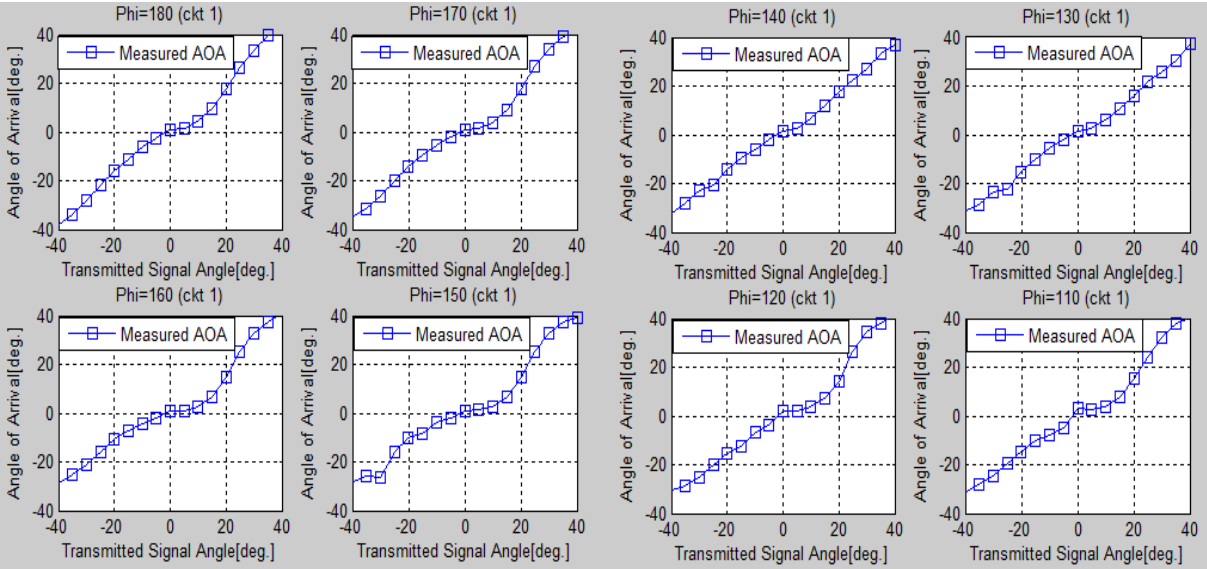
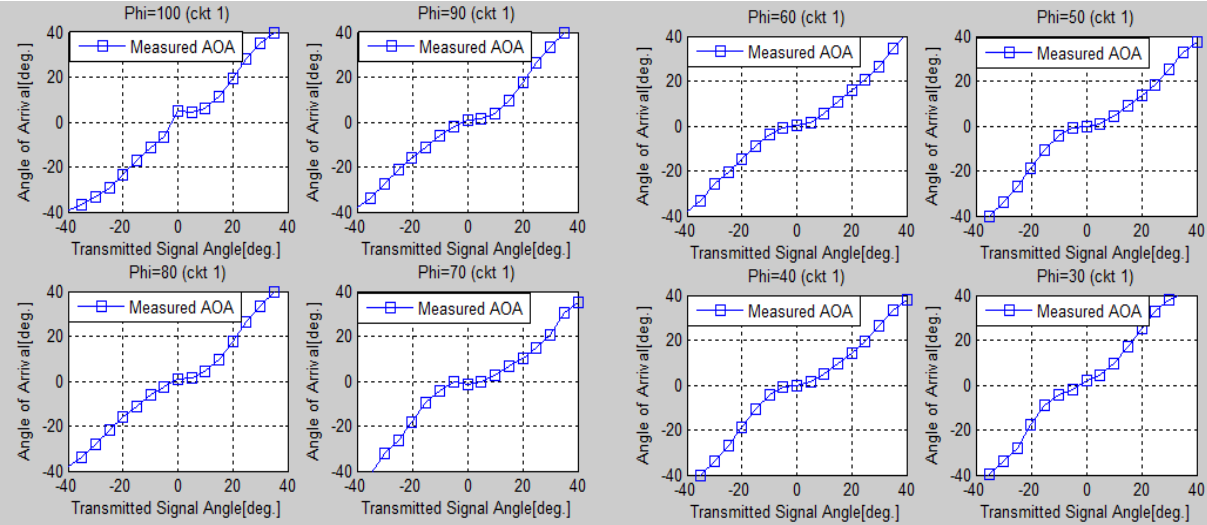


Figure 4-10: Measured Angle of Arrival of received signal of circuit1 (theta axis)

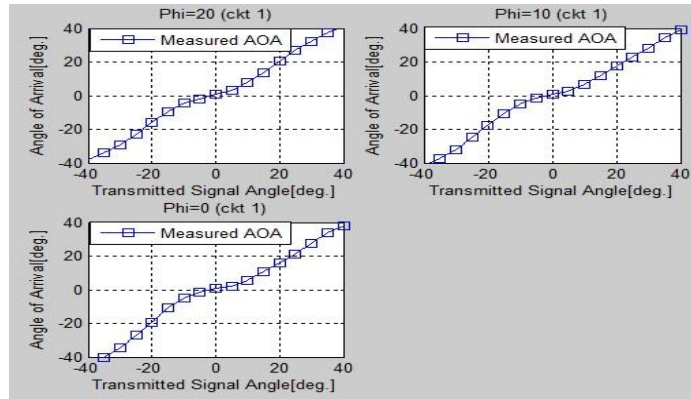
Same circuit has been used to get the 3D radiation pattern from $\theta = -90$ to $+90$ and $\phi = 0$ to 180 degrees. Using this 3D radiation patterns of difference and sum ports in Matlab, AOA has been observed from -40 to $+40$ in θ axis at each value of $\phi = 0$ to 180 with step size of 10 . Note that in every step, each ϕ value has been put constant and DOA has been observed. Figure 4-11 shows the different plots of estimated AOA in θ axis at each ϕ value. Against each ϕ value, rms error has been calculated for the performance measurement of AOA in θ axis. Since this circuit works well to find DOA up-to 40° with rms error less than 5 degrees, so this rms error at each ϕ value (180 to 0 deg.) has been determined and shown in figure 4-12. In order to check the performance of this circuit above 40 degrees, rms error has been calculated by choosing AOA as -60° to $+60^\circ$ and -80° to $+80^\circ$ at each constant ϕ value. This performance is shown in figure 4-13.



a) $\phi = 180$ to 110



b) $\phi = 100$ to 30



c) $\phi=20$ to 0

Figure 4-11: Plots of estimated AOA -40° to 40° in theta axis at different phi value.

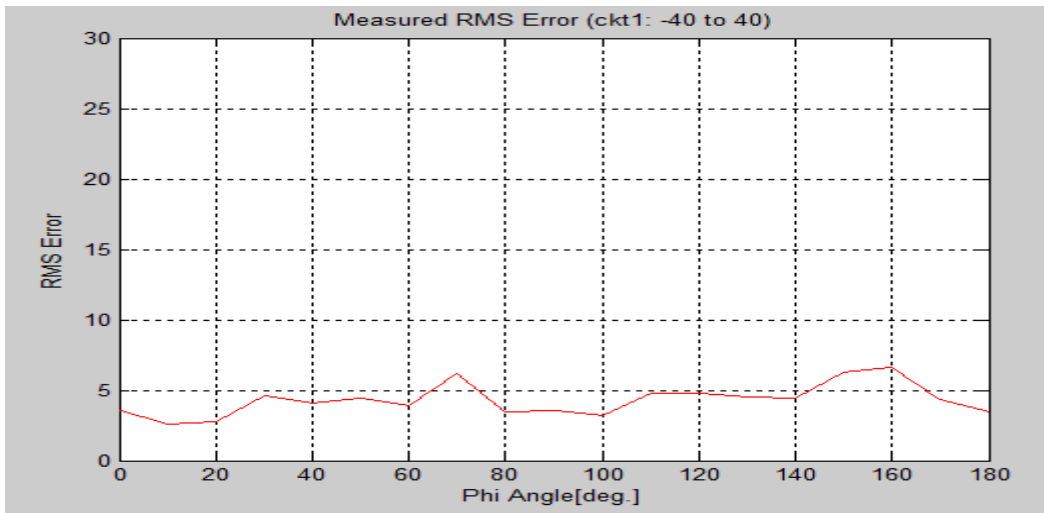


Figure 4-12: RMS error for measured DOA in theta axis (-40° to $+40^\circ$).

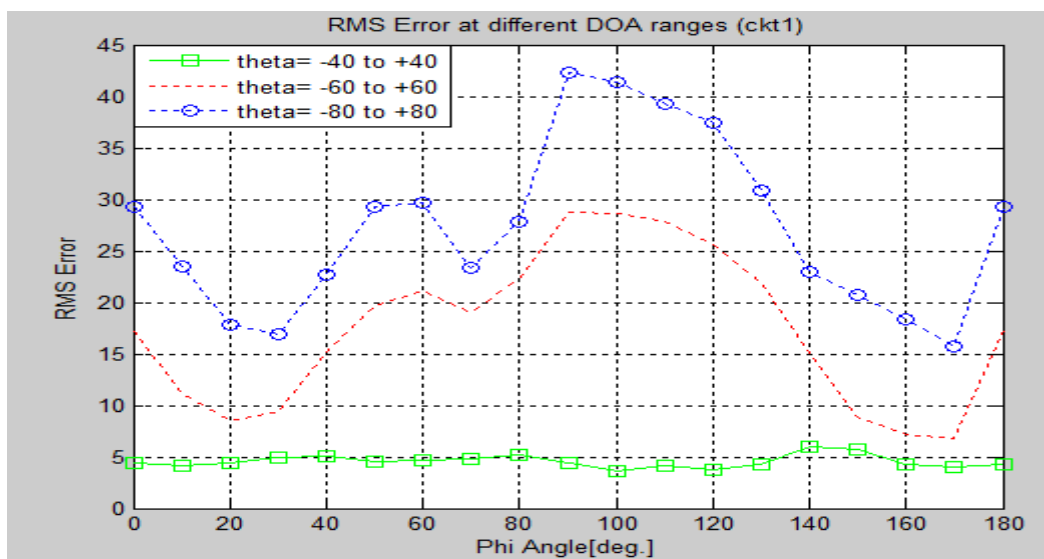


Figure 4-13: RMS error at different DOA ranges in theta axis.

4.3 Estimating DOA in ϕ axis

Similarly like previous circuit, another circuit (circuit 2) which is at 90° than circuit 1 has been designed to obtain DOA in ϕ axis. First, it is designed in ADS layout and simulated for desired results as did for circuit 1 and then fabricated for practical results. ADS layout design of this circuit 2 is shown in figure 4-14. Its simulated S-parameters, far field patterns and antenna parameters are shown in figures 4-15, 4-16, 4-17. In ADS far field simulation, using table 4-1 values, Δ and Σ ports were excited and beam was observed to be moved from 0 to 30 degrees as values of θ varies from 0 to 30 degrees ($\phi=90$), respectively, with approximately $\pm 3^\circ$ error at some θ values. As shown in figure 4-17, gain obtained is 8.89 dBi and directivity 10.13dBi. These simulated results again are in satisfactory range. Later this circuit has been fabricated on same substrate RT Duroid 5880 ($\epsilon_r = 2.2$, *thickness* = 1.575mm). This fabricated circuit is shown in figure 4-18 with SMA connectors soldered from back side. Later the circuit was tested in Anechoic Chamber for measured results in phi axis. Further, using Agilent Network Analyzer (up-to 50GHz), S-parameters and Δ & Σ patterns have been measured which later plotted by importing in Matlab and are shown in figures 4-19 and 4-20. Having, Δ and Σ patterns of experimental setup, angle of arrival in phi axis can be estimated like circuit 1. Similarly as done for circuit 1, a Matlab code is written for this task and angle of arrival from -40 to 40 degrees with rms error of less than 5 degrees has been observed. These values of estimated angle of arrival of received signal v.s actual transmitted signal angles are plotted in Matlab from 0 to 40 degrees and are shown in figure 4-21. Note that written Matlab code for this work is same as given in appendix B.

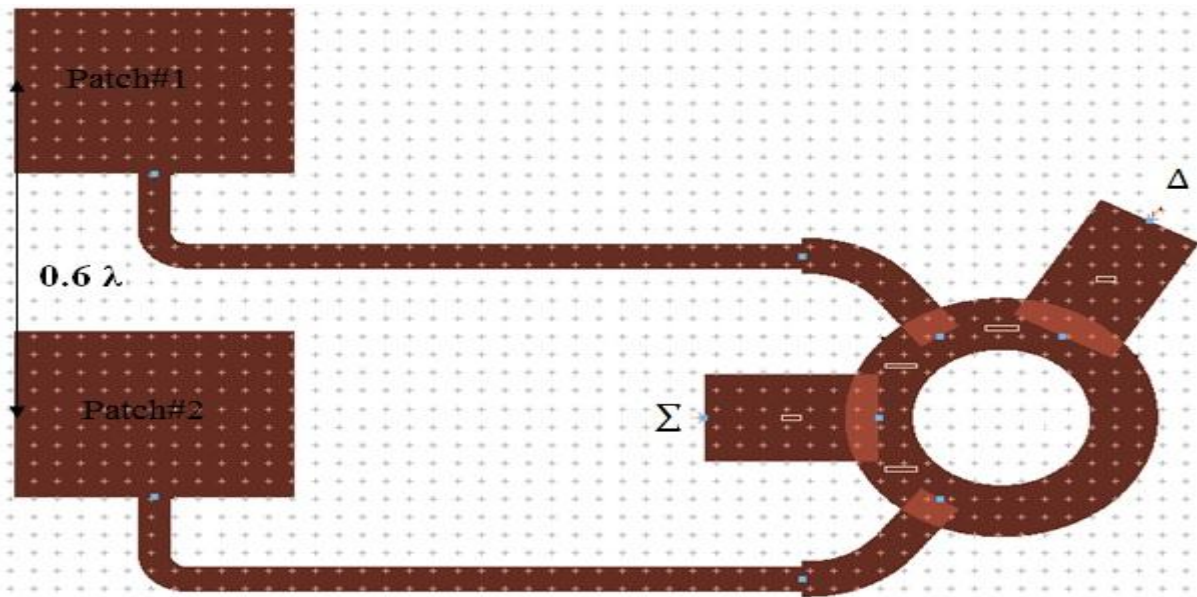


Figure 4-14: ADS layout design of Δ - Σ Pattern, circuit 2 (horizontal)

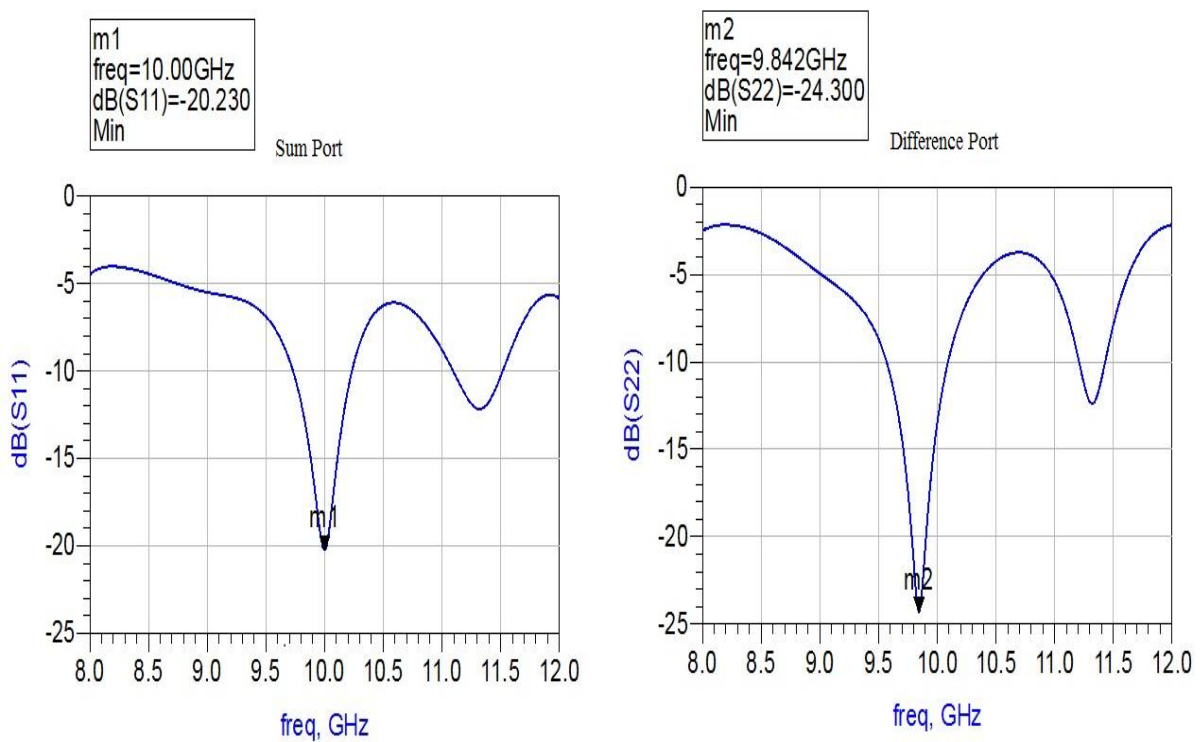
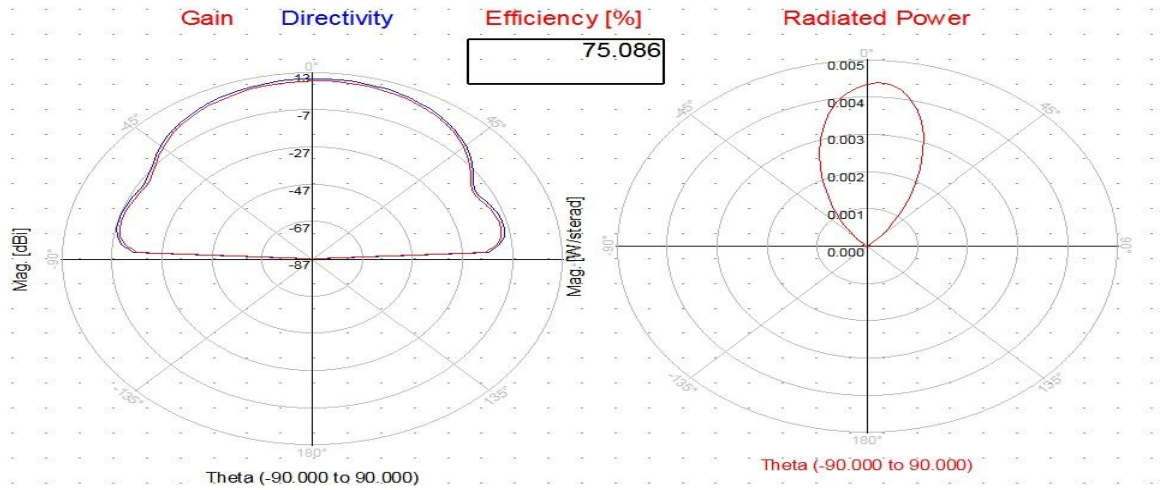
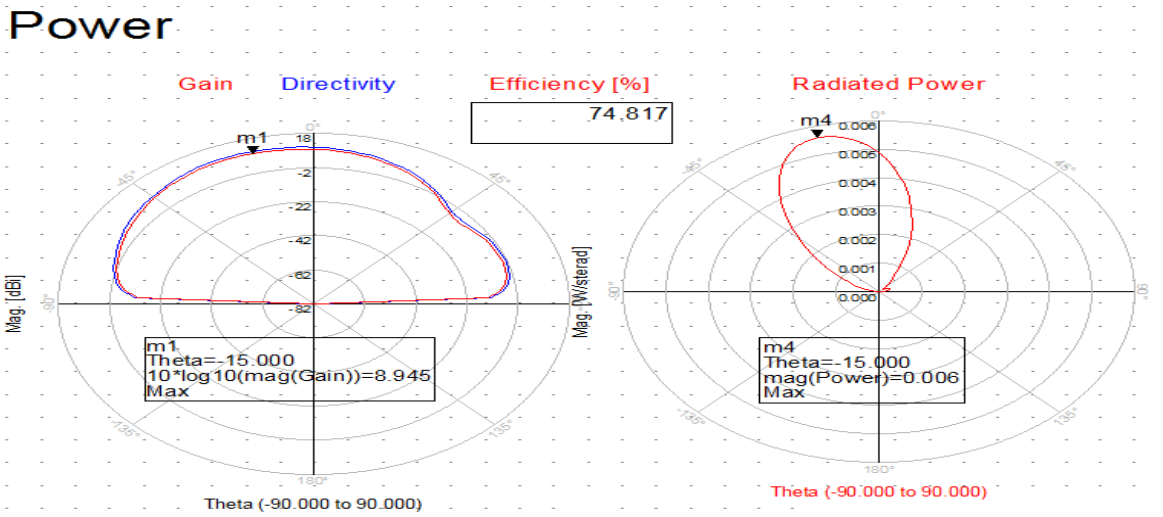


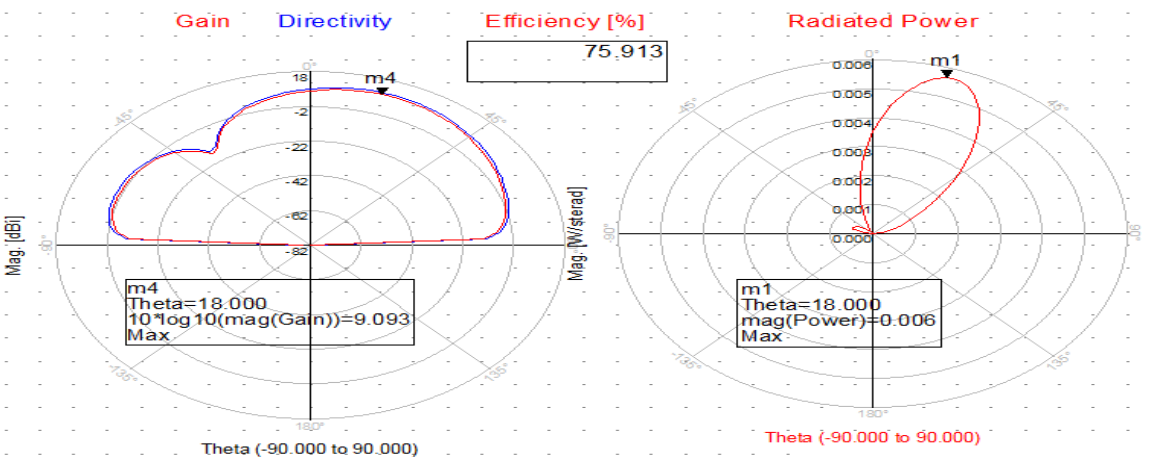
Figure 4-15: S-parameters of Δ and Σ ports, simulated in ADS layout



a) 2D gain and Radiated Power plots at $\theta=0^\circ$



b) 2D gain and Radiated Power plots at $\theta=-15^\circ$



c) 2D gain and Radiated Power plots at $\theta=+15^\circ$

Figure 4-16: Far field patterns at different applied theta values.

| Antenna Parameters | |
|------------------------------|------------|
| Power radiated (Watts) | 0.00597562 |
| Effective angle (Steradians) | 1.21715 |
| Directivity(dBi) | 10.1386 |
| Gain (dBi) | 8.89424 |

Figure 4-17: Antenna parameters

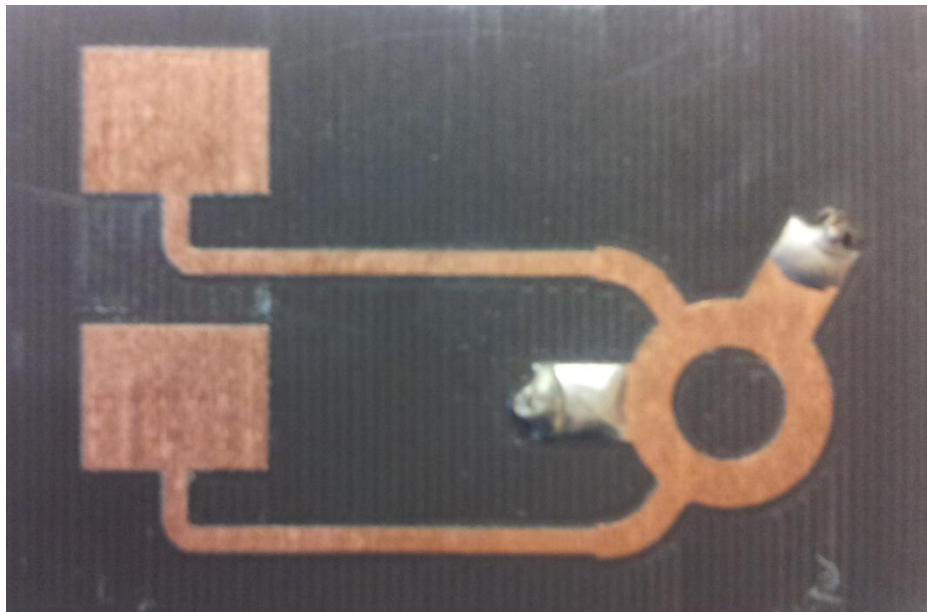


Figure 4-18: Difference – Sum Pattern circuit 2 fabricated (phi axis)

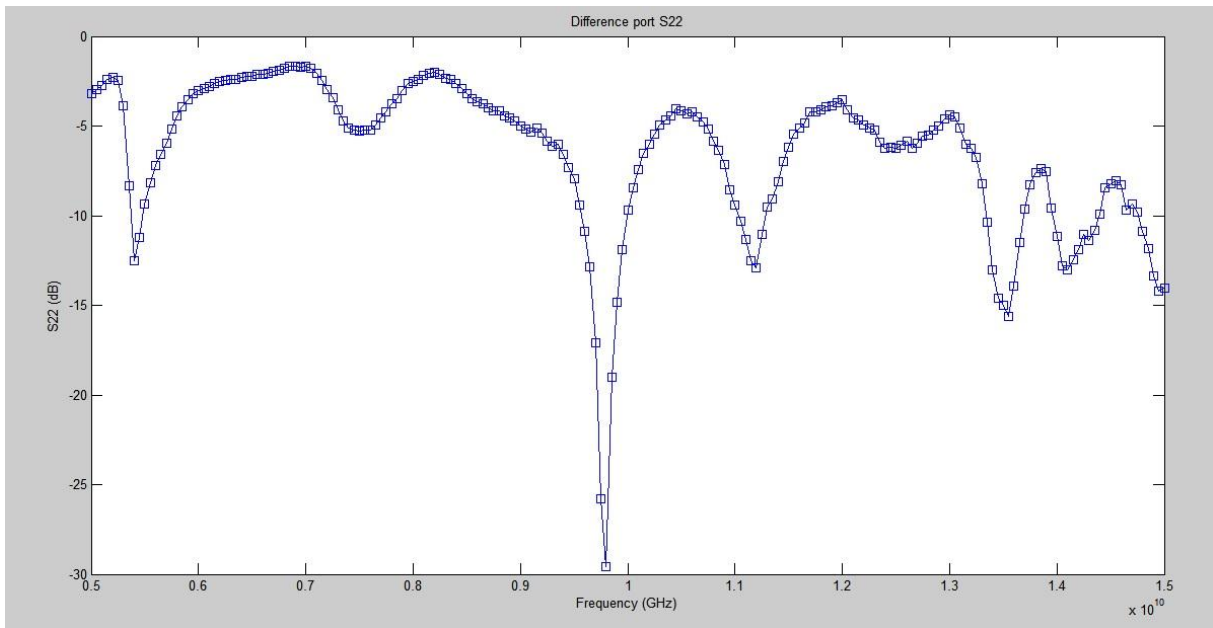
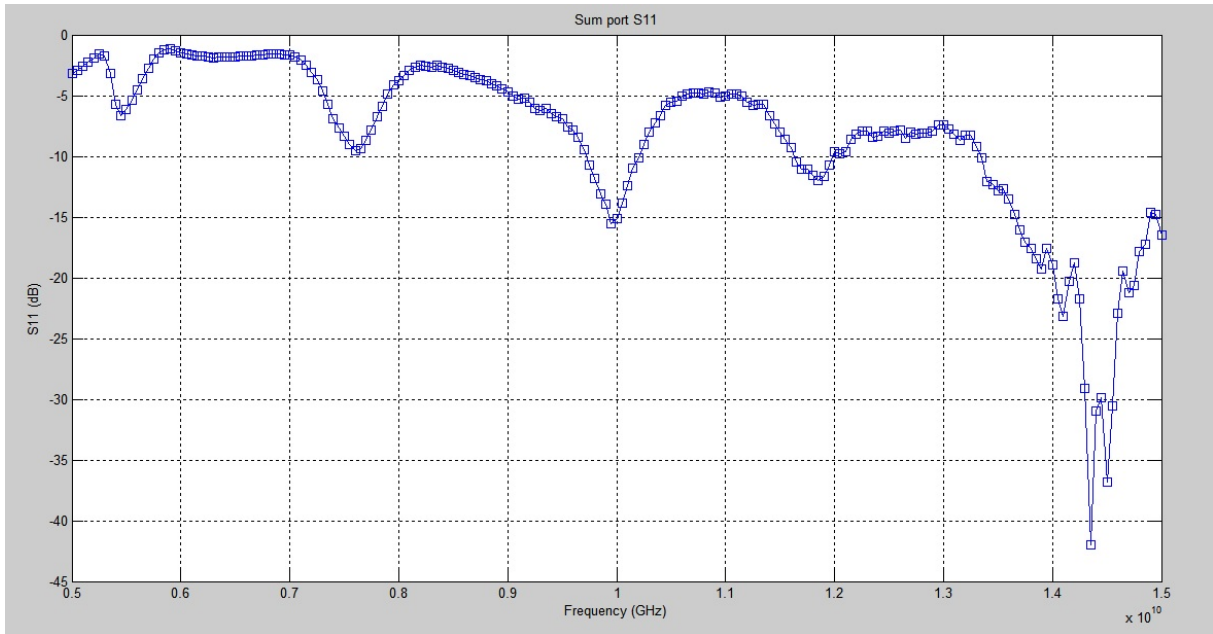


Figure 4-19: Measured S-parameters of Σ and Δ ports, respectively (circuit 2)

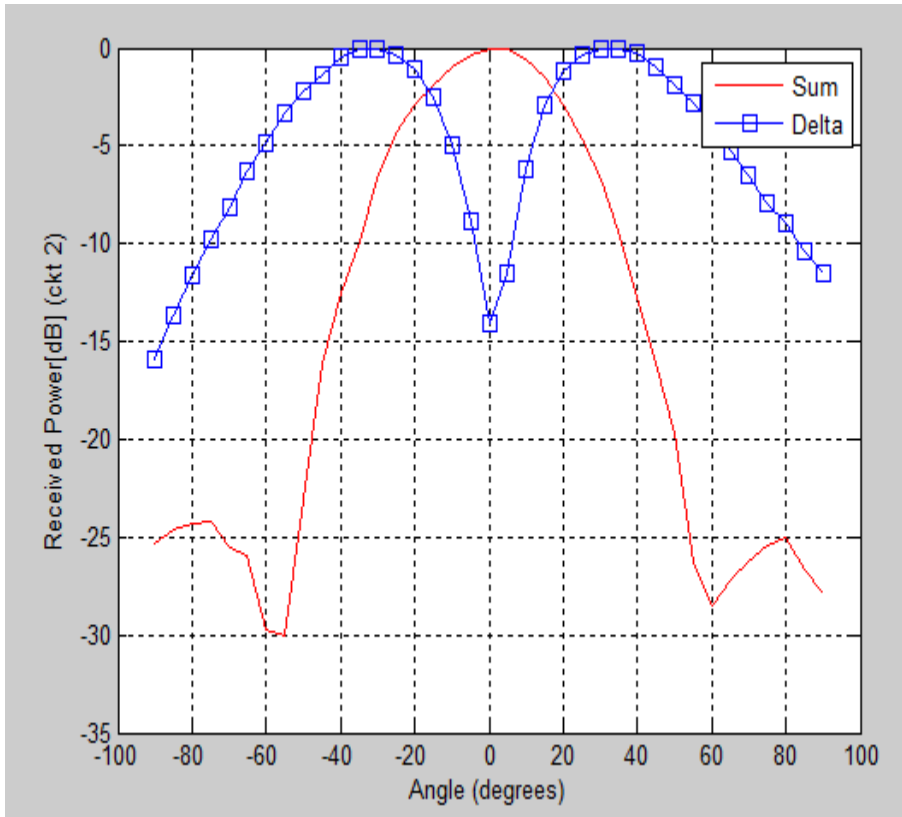


Figure 4-20: Measured normalized Δ and Σ patterns (circuit 2)

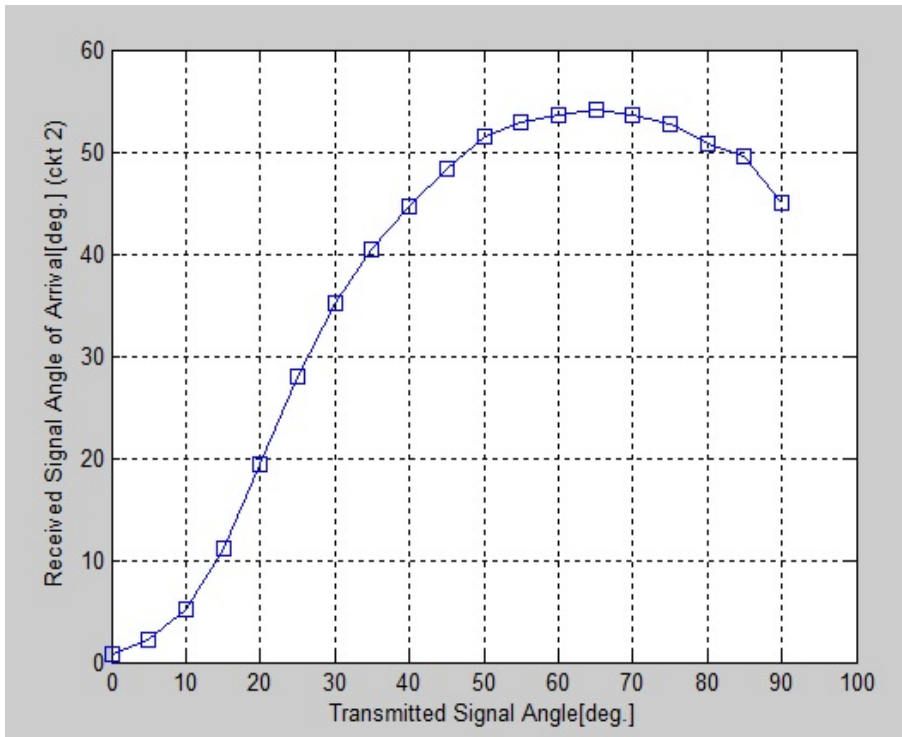
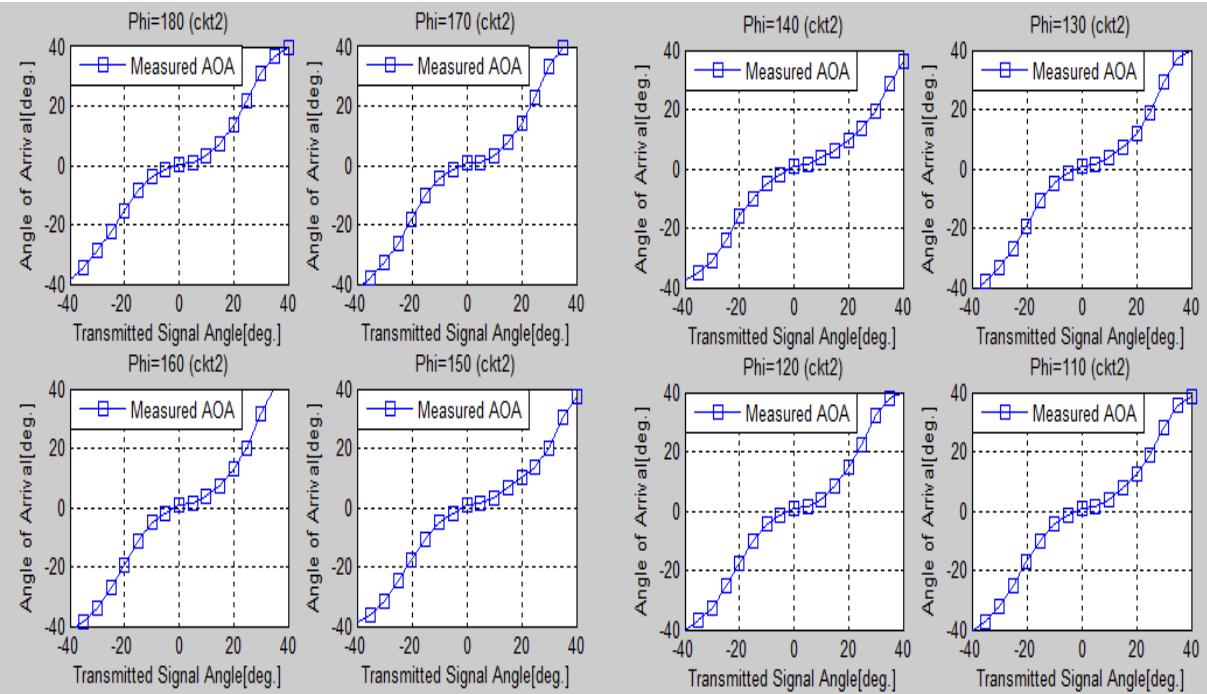


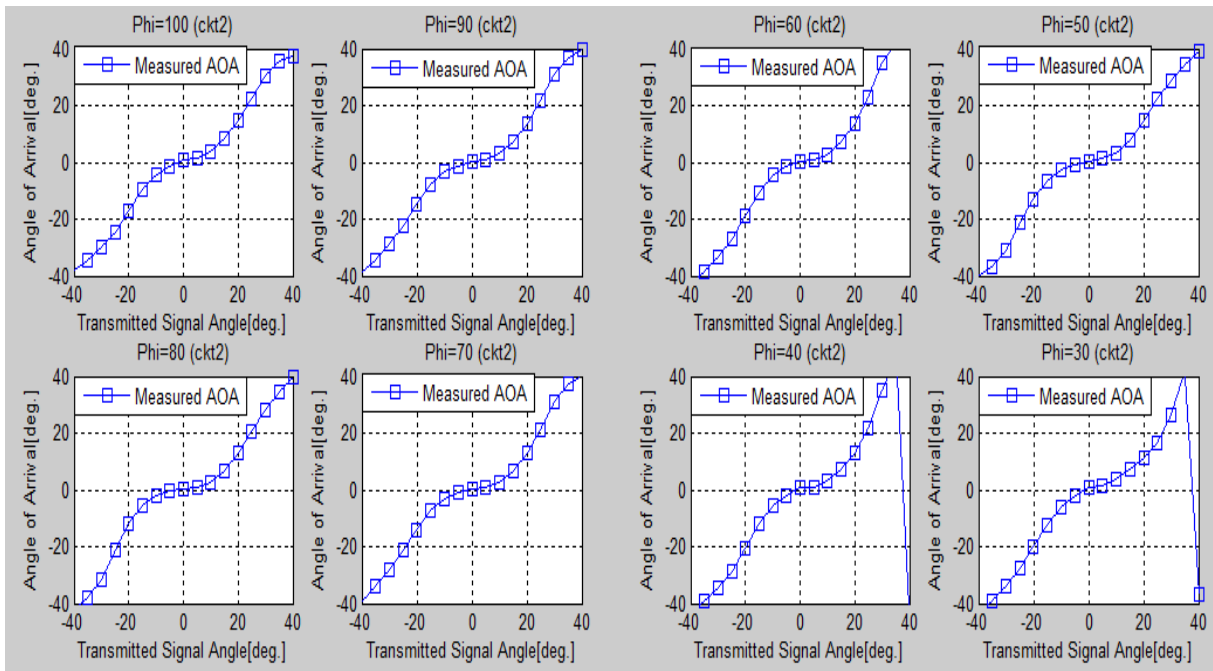
Figure 4-21: Measured Angle of Arrival of received signal of circuit2 (phi axis)

As done for theta axis, same circuit 2 has been used to get the 3D radiation pattern in anechoic chamber. Using this 3D radiation pattern of difference and sum ports in Matlab, AOA has been observed same from -40 to +40 in phi axis as expected at each value of theta = 0 to 180 with step size of 10 (now theta values have become as phi values and hence we call it as AOA in phi axis while phi values have become theta values: 180 to 0 deg.). Note that in every step, each theta value has been put constant and DOA has been observed. Also note that, in both axis (θ, ϕ) obtained DOA is -40 to 40 because both circuits are same but placed at 90° apart. Figure 4-22 shows the different plots of estimated AOA in phi axis at each theta value. Against each theta value, rms error has been calculated for the performance measurement of AOA in phi axis as done for theta axis. Since this circuit works well to find DOA up-to $\pm 40^\circ$ with rms error less than 5 degrees, so this rms error at each constant theta value (180 to 0 deg.) has been determined and shown in figure 4-23. In order to check the performance of this circuit above 40 degrees, rms error has been calculated by choosing AOA as -60° to $+60^\circ$ and -80° to $+80^\circ$ at each constant theta value. This performance is shown in figure 4-24.

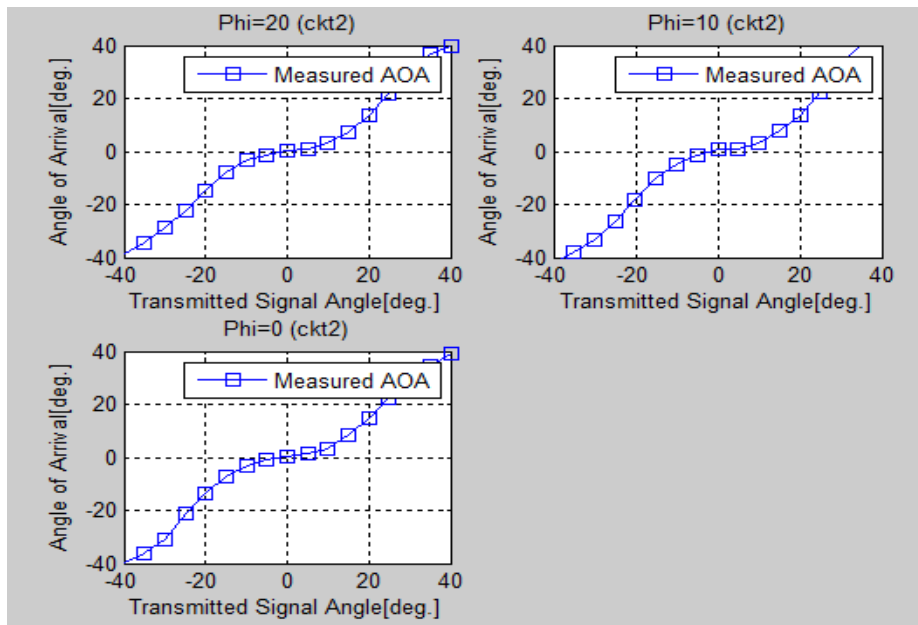
Obtained DOAs in both axis (theta and phi) at fixed phi value are together plotted and shown in figure 4-25.



a) theta = 180 to 110



b) $\theta = 100$ to 30



c) $\theta = 20$ to 0

Figure 4-22: Plots of estimated AOA (-40^0 to 40^0) in phi axis at different theta values.

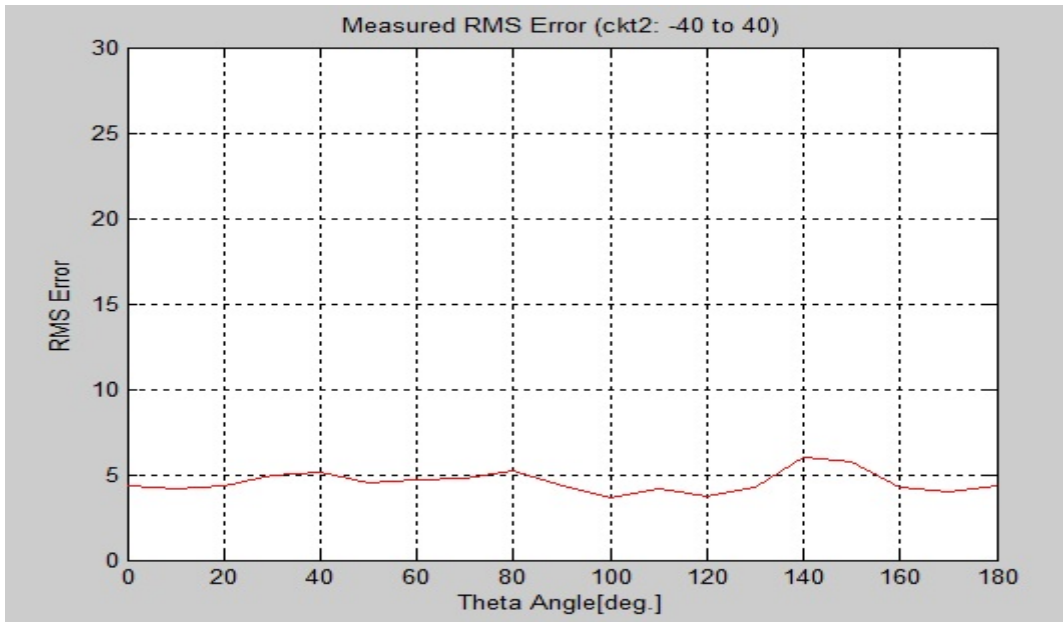


Figure 4-23: RMS error for measured DOA in phi axis (-40⁰ to +40⁰).

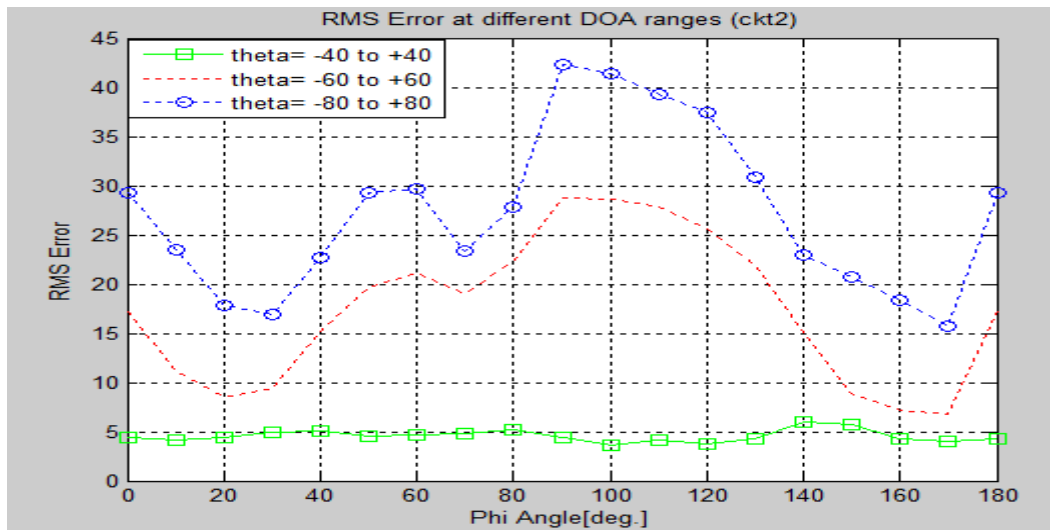


Figure 4-24: RMS error at different DOA ranges in phi axis.

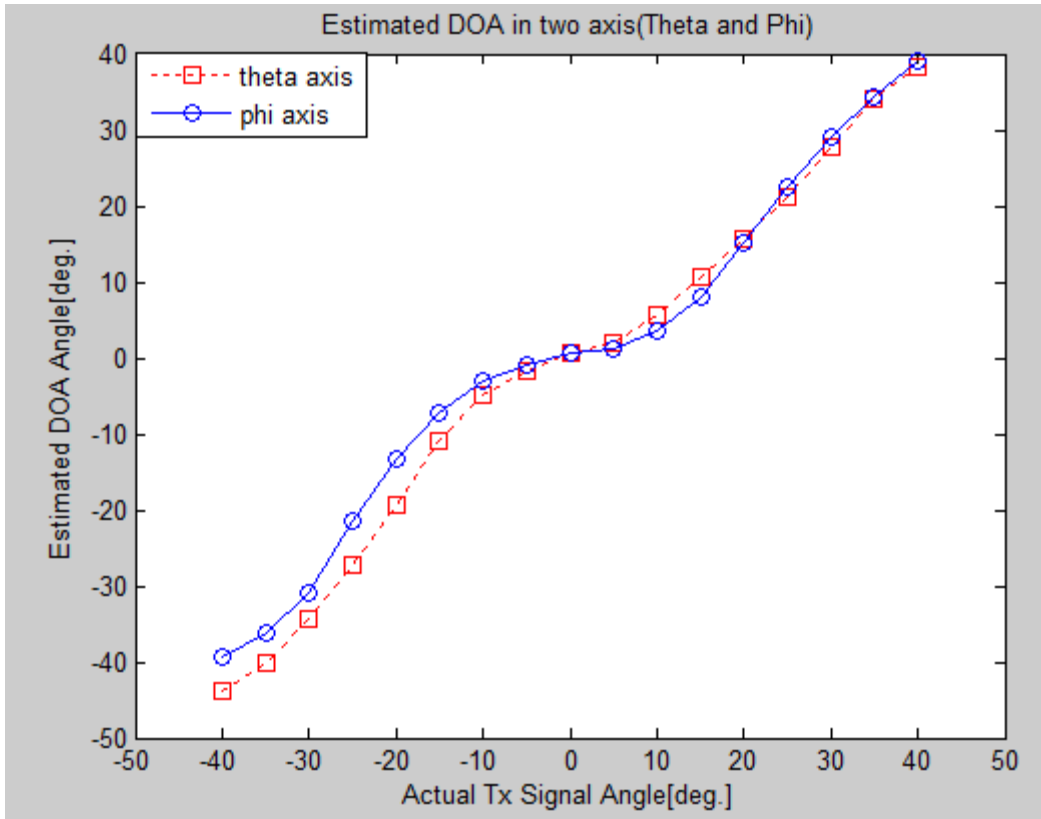


Figure: 4-25: Estimated DOA in both axis (theta and phi) at fixed phi value (0 deg.).

Moreover, as shown in figure 4-26, another circuit which combines all these four antennas into one system also has been simulated in ADS which gives over all system design. Working principle of this design is that we have two sections of same $\Delta - \Sigma$ circuit but in each section both antenna elements are being fed by different locations which result in opposite current directions. So this thing has been compensated by giving one of the elements a phase shift of 180° which has been calculated from below equation (4-2). Therefore, one of the elements transmission line must be 10mm longer than the other element's transmission line.

$$\Delta L = \frac{\Delta\phi}{\beta} = \frac{\Delta\phi}{2\pi} \lambda_g = \frac{\pi}{2\pi} \frac{\lambda_{air}}{\sqrt{\epsilon_r}} = 10\text{mm} \quad (4-2)$$

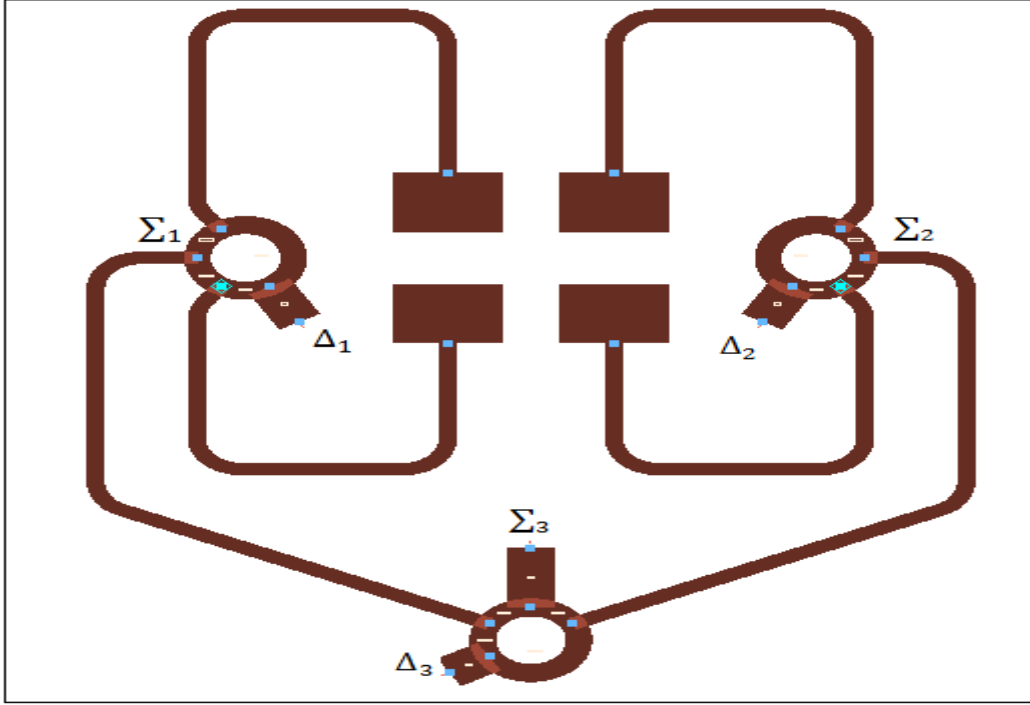


Figure 4-26: Overall system design

Each section can find the DOA in one axis (theta) easily using the procedure as done previously. In order to find the DOA in other axis (phi), we need to take the sum outputs (Σ_1, Σ_2) and apply as two inputs to another coupler in order to take out the difference and sum (Δ_3, Σ_3). Note that in this case one of the applied summation pattern (Σ_1 or Σ_2) must be multiplied by $e^{-jkdsin\phi}$ in order to scan in other axis. Having this information, Σ_1 and Σ_2 patterns are given below in equations (4-3 and 4-4) from which Σ_3 , and Δ_3 pattern equations have been formed by simply adding and subtracting Σ_1 and Σ_2 and are given in equations (4-5 and 4-6). By taking ratio Δ_3 to Σ_3 , DOA angle in phi axis has been driven by performing some mathematical iterations and is given in equation (4-7).

$$\Sigma_1 = 1 + e^{-jkdsin\theta} \quad (4-3)$$

$$\Sigma_2 = (1 + e^{-jkdsin\theta})e^{-jkdsin\phi} \quad (4-4)$$

$$\Sigma_3 = \Sigma_1 + \Sigma_2 \quad (4-5)$$

$$\Delta_3 = \Sigma_1 - \Sigma_2 \quad (4-6)$$

$$\phi = \sin^{-1} \left(\frac{\lambda}{\pi d} \tan^{-1} \frac{\Delta_3}{\Sigma_3} \right) \quad (4-7)$$

5. Conclusion

Direction of arrival (DOA) system having application in radar, sonar, military, acoustic, communication and medical imaging is being widely studied in various communication fields. Researchers are trying to face the requirements of high efficiency, proper functionality and compactness for radars and sensors. By keeping this idea in mind, this thesis work has been carried out to research in DOA system design in order to obtain DOA of received signal using difference (Δ) and sum (Σ) patterns in two axis.

In this thesis work, a direction finding system has been implemented to estimate the DOA of received signal in x-band. Proposed system consists of microstrip patch antenna array of two elements spaced 0.6λ and 180° hybrid rat race coupler which generates the Δ and Σ patterns of two received signals according to equations (2-1 and 2-2). For array part, microstrip patch antenna has been designed for reception of RF signal at 10GHz operating frequency while as part of Δ and Σ pattern, rat race coupler designed and optimized for accurate results at central frequency. Antenna array and coupler were integrated and $\Delta - \Sigma$ patterns obtained, in vertical and horizontal directions, by constructing two separate same design circuits, one for finding AOA in theta axis and other circuit for finding AOA in phi axis. Using these $\Delta - \Sigma$ patterns, angle of arrival (AOA) has been estimated by using equation (2-3). This task first has been analyzed numerically using $\Delta - \Sigma$ equations in Matlab, then designed in ADS layout and simulated. Obtained ADS simulated S-parameters, far field $\Delta - \Sigma$ patterns and antenna parameters are in acceptable range.

Later simulated designs of both circuits were fabricated on RT Duroid 5880 ($\epsilon_r = 2.2$, *thickness* = 1.575mm) substrate by machine etching process. Fabricated circuits were tested in Anechoic Chamber using a horn antenna as a transmitter and constructed circuits as receiving element at 10GHz frequency of operation. Each circuit's 3D ($\theta = -90$ to $+90$, $\phi = 180$ to 0 degrees) Δ and Σ patterns were taken as measured data. Experimentally obtained data was imported in Matlab for analysis of DOA. Measured S-parameters and far field $\Delta - \Sigma$ patterns are very close to simulated results. From $\Delta - \Sigma$ patterns of each circuit, DOA has been estimated for both axis (theta and phi) by using the equation (2-3). Both circuits are able to find angle of arrival from -40 to $+40$ degrees in their respective axis (circuit 1 for theta axis and circuit 2 for phi axis). RMS error also has been calculated at each constant 3D phi value for measured data of DOA from -90 to $+90$ and found as less than 5 degree of rms error for both circuits at -40 to $+40$ while it increases more as we go above the 40 degrees. This suggests that designed DOA works well for 0 to ± 40 degrees. By looking

at all simulated and measured results, proposed system design of DOA works in satisfactory range which in result fulfills the purpose of this thesis work.

As a future work, to improve more results, substrate material can be chosen such that its thickness is lower than this thesis substrate thickness because thicker material introduces more losses at higher frequencies such as x-band frequency spectrum. Moreover, the increase in number of antenna elements can be one possible way towards further improvement. However, this will increase the gain and so the operation range, however size of the antenna array will become significantly large. Another noticeable improvement in results can be achieved if we use another antenna such as dipole, instead of patch antenna because of its narrow beamwidth.

6. Appendices

6.1 Appendix A

Matlab code for numerically analysis of Difference – Sum Pattern and Angle of Arrival

Note that 2D gain pattern values obtained from ADS simulations of single 10GHz patch antenna, can be saved in Microsoft excel (.xlsx) file.

```
clear all;
clc;
close all;
f=10*10^9;
v=3*10^8;
lambda=v/f;
k=(2*pi)/lambda;
d=0.5*lambda;

[n t] = xlsread('D:\Users\SUUSER\Desktop\1elementGainPattern.xlsx');
theta = n(1:62,1);
gainDB = n(1:62,2);

delta=pow2db(abs(1-(exp(-j*k*d*sin(theta)))));
summation=pow2db(abs(1+(exp(-j*k*d*sin(theta)))));

delta(31,1)=-22;
delta(32,1)=-22;
funcOfDelta = delta+gainDB;
funcOfSummation = summation+gainDB;

normalizedDelta=funcOfDelta-max(funcOfDelta);
normalizedSummation=funcOfSummation-max(funcOfSummation);

figure;
plot(theta,normalizedDelta,'s-b');
xlabel('Angle [deg.]);
ylabel('Received Power [dB]);
axis([-90 90 -50 0]);
hold on
plot(theta,normalizedSummation,'-r');
legend('Delta','Sum');
```

```
%finding angle of arrival from 0 to 90
sum1Power=db2pow(normalizedSummation(32:62));
diff1Power=db2pow(normalizedDelta(32:62));
deltaToSumRatio=(diff1Power/sum1Power);
tanInvOfRatio=atan(deltaToSumRatio);
DOA=rad2deg(asin((lamba/(pi*d))*tanInvOfRatio));
theta11=theta(32:62);
```

```
figure ;
plot(theta11, DOA);
xlabel('Angle [deg.]');
ylabel('Direction of Arrival[deg.]');
```

$$\Sigma = 1 + e^{-jkd \sin \theta}$$

Sum of two signals

$$\Delta = 1 - e^{-jkd \sin \theta}$$

difference of two signals

taking ratio of Δ to Σ

$$\frac{\Delta}{\Sigma} = \frac{1 - e^{-jkd \sin \theta}}{1 + e^{-jkd \sin \theta}}$$

$$\left\{ \begin{array}{l} d = \text{Space between two antenna elements} \\ k = \frac{2\pi}{\lambda} \end{array} \right.$$

$$= \frac{e^{-j\frac{kd \sin \theta}{2}} \left(e^{j\frac{kd \sin \theta}{2}} - e^{-j\frac{kd \sin \theta}{2}} \right)}{e^{-j\frac{kd \sin \theta}{2}} \left(e^{j\frac{kd \sin \theta}{2}} + e^{-j\frac{kd \sin \theta}{2}} \right)}$$

$$= \frac{j \sin \left(\frac{kd}{2} \sin \theta \right)}{\cos \left(\frac{kd}{2} \sin \theta \right)}$$

$$= j \tan \left(\frac{kd}{2} \sin \theta \right)$$

$$\tan^{-1} \left(\frac{\Delta}{\Sigma} \right) = \frac{kd}{2} \sin \theta$$

$$\sin \theta = \frac{2}{kd} \tan^{-1} \left(\frac{\Delta}{\Sigma} \right)$$

$$\Rightarrow \theta = \sin^{-1} \left(\frac{2}{kd} \tan^{-1} \left(\frac{\Delta}{\Sigma} \right) \right)$$

$$\theta = \sin^{-1} \left(\frac{\lambda}{\pi d} \tan^{-1} \left(\frac{\Delta}{\Sigma} \right) \right)$$

Angle of Arrival (AOA)
of Direction of Arrival (DOA)

6.2 Appendix B

Matlab code estimating theta/phi axis using difference – sum patterns

```
clear all;
clc;
close all;

c=3*10^8;
f=10*10^9;
lambd=c/f;
d=0.6*lambd

[n1 t1] = xlsread('D:\Users\SUUSER\Desktop\ckt1RadPattern1SumPort.xlsx');
[n2 t2] = xlsread('D:\Users\SUUSER\Desktop\ckt1RadPattern2SumPort.xlsx');
[n3 t3] = xlsread('D:\Users\SUUSER\Desktop\ckt2RadPattern1DiffPort.xlsx');
[n4 t4] = xlsread('D:\Users\SUUSER\Desktop\ckt2RadPattern2DiffPort.xlsx');

angle1 = n1(1:37,1);

sum1Amp = n2(1:37,2);
max_sum1Amp =max(sum1Amp)
sum1AmpNormalized=sum1Amp-max_sum1Amp;

diff1Amp = n4(1:37,2);
max_diff1Amp = max(diff1Amp)
diff1AmpNormalized=diff1Amp-(max_diff1Amp);

figure ;
plot(angle1,sum1AmpNormalized,'-r');
xlabel('Angle (degrees)');
ylabel('Received Power[dB] (ckt 2)');
grid on;
hold on;
plot(angle1,diff1AmpNormalized,'s-b');
legend('Sum','Delta');

sum1Power=db2pow(sum1AmpNormalized(19:37));
diff1Power=db2pow(diff1AmpNormalized(19:37));
angle11=angle1 (19:37);

deltaToSumRatio=(diff1Power./sum1Power);
tanInvOfRatio=atan(deltaToSumRatio);
AOA=rad2deg(asin((lambd/(pi*d))*tanInvOfRatio));

figure ;
plot(angle11,AOA, 's-b');
xlabel('Transmitted Signal Angle[deg.]');
ylabel('Received Signal Angle of Arrival[deg.] (ckt 2)');
grid on;
```

```

hold on;
error=(angle11-AOA)
plot(angle11,error, '-r');
grid on;
legend ('Estimated DOA ', 'Error');

sum1Power2=db2pow(sum1AmpNormalized);
diff1Power2=db2pow(diff1AmpNormalized);
deltaToSumRatio2=(diff1Power2./sum1Power2);
tanInvOfRatio2=atan(deltaToSumRatio2);
AOA2=rad2deg(asin(lambda/(pi*d)*tanInvOfRatio2));
figure ;
plot(AOA2(19:37),deltaToSumRatio2(19:37), 's-b');
xlabel('Arrival angle[deg.]');
ylabel('Delta/Sum (ckt 2)');
grid on;

```

6.3 Appendix C

Finding Difference – Sum absolute and phase values using equations (2-1 and 2-2) in order to excite the ports of ADS

```

clear all;
clc;
close all;

c=3*10^8;
f=10*10^9;
lambda=c/f;
d=0.6*lambda
d1=0.6*lambda;
k=(2*pi)/lambda
kd=k*d;

theta1= -pi/4:pi/12:pi/4;
phi1= 0

sum1=1+exp(-j*(kd)*sin(theta1));
sum1abs=abs(sum1);
sum1phase=rad2deg(phase(sum1));

delta1=1-exp(-j*(kd)*sin(theta1));
delta1abs=abs(delta1);
delta1phase=rad2deg(phase(delta1));

sum2= (1+exp(-j*(kd)*sin(theta1)))*(exp(-j*k*sin(phi1)));
sum2abs=abs(sum2);
sum2phase=rad2deg(phase(sum2));

```

```
delta2=(1-exp(-j*(kd)*sin(theta1)))*(exp(-j*k*sin(phi1)));  
delta2abs=abs(delta2);  
delta2phase=rad2deg(phase(delta2));
```

```
sum3=(1+exp(-j*(kd)*sin(theta1)))*(1+exp(-j*k*sin(phi1)));  
sum3abs=abs(sum3);  
sum3phase=rad2deg(phase(sum3));
```

```
delta3=(1+exp(-j*(kd)*sin(theta1)))*(1-exp(-j*k*sin(phi1)));  
delta3abs=abs(delta3);  
delta3phase=rad2deg(phase(delta3));
```

7. References

- [1] A.Vesa, G.Iozsa, “Direction – of – Arrival Estimation for Uniform Sensor Arrays”, IEEE Electronics and Telecommunications (ISETC), 2010.
- [2] Ryo Tanaka, Eisuke Nishiyama, and Ichihiko Toyoda, “A Mono-Pulse DOA Estimation Antenna Integrated with RF Amplifiers and Detection Circuits”, IEEE Antennas and Propagation Society International Symposium (APSURSI), July 2014.
- [3] M. Rubsamen and A. Gershman, “Direction – of – Arrival for Nonuniform Sensor Arrays: From Manifold Separation to Fourier Domain MUSIC Methods,” IEEE Transactions on Signal Processing, vol. 57, no. 2, pp. 588 – 599, February 2009.
- [4] L. Yip, K. Comanor, J. C. Chen, R. E. Hudson, K. Yao, and L. Vandenberghe, “Array Processing for Target DOA, Localization, and Classification Based on AML and SVM Algorithms in Sensor Networks,” Information Processing in Sensor Networks, Lecture Notes in Computer Science, Vol. 2634, pp. 269-284, Springer, 2003.
- [5] Warren L.Stutzman & Gary A. Thiele, “Antenna Theory and Design”, edition 2, John Wiley & Sons Inc, Newyork 1998.
- [6] Hirotoishi Sakai, Eisuke Nishiyama, and Ichihiko Toyoda, “Direction of arrival estimating array antenna”, Proceedings of ISAP2012, Nagoya, Japan, 2012.
- [7] Constantine A. Balanis, “Antenna Theory, Analysis and Design”, edition 2, John Wiley & Sons Inc, Newyork, 1997.
- [8] Telecom Hall, ‘What is Antenna’, (<http://www.telecomhall.com/what-is-antenna.aspx>), November 20, 2014.
- [9] Beamwidths and Sidelobe Levels, ‘Antenna Fundamentals’, (<http://www.antenna-theory.com/basics/radPatDefs.php>), November 24, 2014.
- [10] Jagdish. M. Rathod, “Comparative Study of Microstrip Patch Antenna for Wireless Communication Application”, International journal of innovation, Management and Technology, Vol 1,No.2,2010.
- [11] Kin-Lu Wong, “Compact and Broadband Microstrip Antennas”, Jon Wiley & Sons, Inc.,2002
- [12] D.M.Pozar and B.Kaufman,”Increasing the Bandwidth of a Microstrip Antenna by Proximity Coupling”, Electronic Letters, Vol- 23, pp [12-14] April-1987.
- [13] G.A. Desschamps, “Microstrip microwave antennas”, presented at the 3d USAF Symposium on Antennas, 1953.
- [14] J.Q. Howell, “Microstrip antennas”, IEEE APS Int. Symposium. Digest, pp. 177-180, 1972.
- [15] Inder J.Bahl, Parkash Bhartia, Stanislaw S. Stuchly, “Design of microstrip antennas Covered with a Dielectric Layer”, IEEE Trans. Antenna Propagation, vol. AP-30, no.2, pp.314-318, March 1982.
- [16] Microstrip Patch Antenna Calculator, (<http://www.emtalk.com/mpacalc.php>), July 01,2014.

- [17] E. Levine, G. Malamud, and S. Shrikman, "A study of microstrip array antennas with the feed network", *IEEE Trans. Antennas Propagation*, vol. 37, pp 426-434, April 1989.
- [18] Antenna Arrays, 'Antenna Theory', (<http://www.antenna-theory.com/arrays/main.php#phased>), November 2014.
- [19] R.E. Munson, "Conformal microstrip antennas and microstrip phased array", *IEEE Trans. Antenna Propagation*, vol. AP-22, pp. 74-78, 1974.
- [20] J. John Huang, "A technique for an array to generate circular polarization with linearly polarized elements", *IEEE Trans. Antenna Propagation*, vol. AP-34, pp. 1113-1124, Sept. 1986.
- [21] Wu, Y., Y. Liu, and S. Li, "Dual-band modified Wilkinson power divider without transmission line stubs and reactive components", *Progress In Electromagnetic Research*, Vol. 96, 393-411, 2009.
- [22] D. M. Pozar, John, "Microwave Engineering," 2nd ed., *Wiley & Sons*, pp. 160-163, 1998.
- [23] T. Johnson and H. Neill, "Complete Mathematics", *Hachette UK Company*, pp.218-220, 2010.
- [24] E. Detsch, A. D. Polyandin and A. I. Chernoutsan, "A Concise Handbook of Mathematics, Physics, and Engineering Sciences", *CRC Press Taylor and Francis Group*, pp. 48, 2011.